The University of Alberta
Printing Department
Edmonton, Alberta

THE UNIVERSITY OF ALBERTA

POINT-MATCHING SOLUTIONS FOR A CLASS OF BOUNDARY-VALUE PROBLEMS USING BIHARMONIC FUNCTIONS IN CARTESIAN COORDINATES

by

YIH-RENN KAN, B.Sc.

(Cheng Kung University)

A THESIS

SUBMITTED TO THE FACULTY OF GRADUATE STUDIES

IN PARTIAL FULFILMENT OF THE REQUIREMENTS FOR THE

DEGREE OF MASTER OF SCIENCE

DEPARTMENT OF MECHANICAL ENGINEERING

EDMONTON, ALBERTA

APRIL 1968

UNIVERSITY OF ALBERTA

FACULTY OF GRADUATE STUDIES

The undersigned certify that they have read, and recommend to the Faculty of Graduate Studies for acceptance, a thesis entitled "POINT-MATCHING SOLUTIONS FOR A CLASS OF BOUNDARY-VALUE PROBLEMS USING BIHARMONIC FUNCTIONS IN CARTESIAN COORDINATES", submitted by YIH-RENN KAN in partial fulfilment of the requirements for the degree of Master of Science.

ABSTRACT

In this thesis, the general solution of the biharmonic equation in Cartesian coordinates is used to solve the following problems:

1. Uniformly loaded rectangular plates with all edges clamped.
2. Uniformly loaded rhombus plates with all edges clamped.
3. Uniformly and hydrostatically loaded circular segmental plates with all edges clamped.
4. Uniformly loaded circular plates with diametrically opposite flat sides and all edges clamped.
5. Creeping flow in rectangular cavities.
6. Creeping flow in triangular cavities.
7. Creeping flow in circular segmental cavities.

The general solution of the biharmonic equation is written in terms of infinite series of harmonic and biharmonic functions which are derived by using the complex-variable method. The coefficients of the infinite series are determined by point-matching technique.

The numerical results have been compared with the available solutions in the literature. It is seen that the numerical results of the present analysis are very satisfactory.

The purpose of this thesis is to show that a class of boundary-value problems can be approached by using biharmonic functions in Cartesian coordinates.

ACKNOWLEDGEMENTS

The author wishes to extend his appreciation to

- Dr. K.C. Cheng for his supervision of this thesis,
- Dr. G. Ford for his guidance during the graduate studies at the University of Alberta,
- The National Research Council of Canada for financial support under grant NRC A-1655 (Cheng),
- Mr. D. Walkingshaw and Mrs. G. Gillespie for their reading the manuscript.

TABLE OF CONTENTS

PAGE

LIST OF FIGURES

FIGURE PAGE

LIST OF TABLES

NOTATIONS

A	Aspect ratio of rectangular cavity (=H/a).
A_m, B_m, C_m, D_m	Coefficients of the general solution of biharmonic equation in polar coordinates.
a_{mn}	Coefficient of the series solution of the biharmonic equation in doubly infinite series.
a	Length dimension in x-direction.
b	Length dimension in y-direction.
b_i	Coefficient of the biharmonic function G_i.
c_i	Coefficient of the harmonic function g_i.
D	$= Et^3/12(1-\mu^2)$, Flexural rigidity of a plate.
E	Modulus of Elasticity.
G_i	Biharmonic function.
g_i	Harmonic function.
H	Depth of the rectangular cavity.
k, ℓ	Real numbers.
M_x, M_y, M_n	Bending moments per unit length of sections of a plate perpendicular to X axis, Y axis and unit normal, respectively.
n	Outward normal of the boundary.
q, q_o	Load intensity.
p_n, q_n, r_n, s_n	Real constants.
M, N, P	Positive integers.
R	Reynolds number.
s	Length dimension in y-direction or along the boundary.

V_o	Velocity of the moving wall for creeping flow problem.
v	Velocity of the creeping flow problem.
w	Deflection of the plate.
ψ	Stream function of the creeping flow problem.
ψ_n	Complex constant.
ϕ_n	Complex constant.
μ	Poisson's ratio (= 0.3 for all the numerical results of the plate problem).

CHAPTER I

INTRODUCTION

1.1 Plate Equation and Its Solutions

The governing differential equation of a laterally loaded thin plate subjected to small deflections is

$$\nabla^4 w = \frac{\partial^4 w}{\partial x^4} + 2\frac{\partial^4 w}{\partial x^2 \partial y^2} + \frac{\partial^4 w}{\partial y^4} = \frac{q}{D} \qquad (1)$$

In the case of a clamped edge the boundary conditions are

$$w = 0 \quad \text{and} \quad \frac{\partial w}{\partial n} = 0, \quad \text{where n is outward normal.}$$

The general solution of differential equation (1) can be written as,

$$w = w_h + w_p ,$$

where w_p is a particular integral of the differential equation (1) and w_h is the solution of the homogeneous biharmonic differential equation

$$\nabla^4 w_h = 0 .$$

The general series solution of the homogeneous biharmonic equation in polar coordinates is [1],

$$w_h = A_o + B_o r^2 + C_o \log r + D_o r^2 \log r$$
$$+ (A_1 r + B_1 r^3 + C_1 r^{-1} + D_1 r \log r) \cos \theta$$

$$+ (A_1' r + B_1' r^3 + C_1' r^{-1} + D_1' r \log r) \sin\theta$$

$$+ \sum_{m=2}^{\infty} (A_m r^m + B_m r^{-m} + C_m r^{m+2} + D_m r^{-m+2}) \cos m\theta$$

$$+ \sum_{m=2}^{\infty} (A_m' r^m + B_m' r^{-m} + C_m' r^{m+2} + D_m' r^{-m+2}) \sin m\theta \qquad (2)$$

This series solution (2) has been successfully used by Conway [2], Cheng [3], Hulbert [4], Lo [5] and many others to solve the elasticity, plate and heat transfer problems where the coefficients A_m, B_m, C_m, D_m, A_m', B_m', C_m' and D_m' were determined by the point matching technique.

It appears that the general solution of the biharmonic equation in Cartesian coordinates was first given by Thorne [6]. Sparrow and Haji-Sheikh [7] set up the general solution of the biharmonic equation in terms of G_i[1] and g_i, where g_i's and G_i's are harmonic and biharmonic functions respectively. Sparrow and Haji-Sheikh have used these functions g_i and G_i to solve the flow and heat transfer in ducts with arbitrary thermal boundary conditions. In this thesis, the general solution of the biharmonic equation in Cartesian coordinates will be derived by complex variable method and polynomial method. It is noted that the functions G_i's obtained are not completely identical with those given in Reference [7].

---

[1] Derivation of the biharmonic function G_i was not discussed in [7].

1.2 Purpose and Problems

The general solution of the biharmonic equation in Cartesian coordinates was first used successfully by Sparrow and Haji-Sheikh [7] in solving laminar forced convection heat transfer problem. The purpose of this thesis is to show that the general solution of biharmonic equation in Cartesian coordinates can be used to solve the plate and creeping flow problems governed by biharmonic equations. It is noted that these functions G_i and g_i have not been used in solving these problems in the past. Approximate solutions are found by employing point-matching technique to obtain the coefficients of the functions g_i and G_i for the following plate and creeping flow problems:

1. Uniformly loaded rectangular plates with all edges clamped.
2. Uniformly loaded rhombus plates with all edges clamped.
3. Uniformly and hydrostatically loaded circular segmental plates with all edges clamped.
4. Uniformly loaded circular plates with diametrically opposite flat sides and all edges clamped.
5. Creeping flow in rectangular cavities.
6. Creeping flow in triangular cavities.
7. Creeping flow in circular segmental cavities.

It is noted that some of the problems mentioned above cannot readily be handled by using the general solution of the biharmonic equation in polar coordinates. Those problems are clamped uniformly loaded rectangular plate with large aspect ratio and clamped uniformly loaded rhombus plate with small angle α.

CHAPTER II

THEORETICAL ANALYSIS

2.1 Derivation of the Biharmonic Function G_i^1 and Harmonic Function g_i^1 by Complex Variable Method

The differential equation (1) in complex coordinate system $(z, \bar{z})$ can be written as;

$$\frac{\partial^4 \tilde{w}(z, \bar{z})}{\partial z^2 \, \partial \bar{z}^2} = \frac{1}{16D} \tilde{q}(z, \bar{z}) \tag{3}$$

where $z = x + iy$, $\bar{z} = x - iy$, $i = \sqrt{-1}$

$$\tilde{w}(z, \bar{z}) = w\left(\frac{z + \bar{z}}{2}, \frac{z - \bar{z}}{2i}\right) = w(x, y) \quad \text{and}$$

$$\tilde{q}(z, \bar{z}) = q\left(\frac{z + \bar{z}}{2}, \frac{z - \bar{z}}{2i}\right) = q(x, y) .$$

It is noted that $\tilde{w}(z, \bar{z})$ and $\tilde{q}(z, \bar{z})$ are both real functions. The general solution of equation (3) is [8],

$$\tilde{w}(z, \bar{z}) = \frac{1}{16D} \iiiint \tilde{q}(z, \bar{z}) \, dz \, dz \, d\bar{z} \, d\bar{z}$$

$$+ \bar{z} \, \Phi(z) + z \, \bar{\Phi}(\bar{z}) + \Psi(z) + \bar{\Psi}(\bar{z}) .$$

Here, $[\bar{z} \, \Phi(z) + z \, \bar{\Phi}(\bar{z})]$ and $[\Psi(z) + \bar{\Psi}(\bar{z})]$

are biharmonic and harmonic functions, respectively.

---

1. See Appendix 1 for forms of g_i and G_i.

Let $\tilde{w}(z, \bar{z}) = \tilde{w}_h + \tilde{w}_p$,

where

$$\tilde{w}_p = \frac{1}{16D} \iiiint \tilde{q}(z, \bar{z})\, dz\, dz\, d\bar{z}\, d\bar{z}$$

$$\tilde{w}_h = \bar{z}\, \Phi(z) + z\, \bar{\Phi}(\bar{z}) + \Psi(z) + \bar{\Psi}(\bar{z}). \qquad (3A)$$

Here, $\Phi(z)$ and $\Psi(z)$ are analytic functions which can be written in the following forms;

$$\Phi(z) = \sum_{n=1}^{\infty} \phi_n z^n$$

$$\Psi(z) = \sum_{n=0}^{\infty} \psi_n z^n$$

where ϕ_n and ψ_n are unknown complex constants. Now, ϕ_n and ψ_n can be written as;

$$\phi_n = p_n + iq_n$$

$$\psi_n = r_n + is_n$$

where p_n, q_n, r_n and s_n are unknown real constants.

Equation (3A) can be expanded as,

$$\tilde{w}_h(z, \bar{z}) = (x - iy) \sum_{n=1}^{\infty} (p_n + iq_n)(x + iy)^n$$

$$+ (x + iy) \sum_{n=1}^{\infty} (p - iq_n)(x - iy)^n$$

$$+ \sum_{n=0}^{\infty} (r_n + is_n)(x + iy)^n + \sum_{n=0}^{\infty} (r_n - is_n)(x - iy)^n$$

$$= 2p_1(x^2 + y^2) + 2p_2(x^3 + y^2x) - 2q_2(x^2y + y^3) + 2p_3(x^4 - y^4)$$

$$- 4q_3(x^3y + xy^3) + (x - iy)\sum_{n=4}^{\infty}(p_n + iq_n)(x + iy)^n$$

$$+ (x + iy)\sum_{n=4}^{\infty}(p_n - iq_n)(x - iy)^n + 2r_o + 2r_ox - 2s_1y$$

$$+ 2r_2(x^2 - y^2) - 4s_2xy + \sum_{n=3}^{\infty}(r_n + is_n)(x + iy)^n$$

$$+ \sum_{n=3}^{\infty}(r_n - is_n)(x - iy)^n .$$

Finally, $\tilde{w}_h(z, \bar{z})$ can be written as;

$$\tilde{w}_h(z, \bar{z}) = 2p_1G_1 + 2p_2G_2 - 2q_2G_3 + 2p_3G_4 - 4q_3G_5$$

$$+ \sum_{n=6}^{\infty}\begin{pmatrix} kp_i \\ \text{or} \\ kq_i \end{pmatrix} G_n + 2r_og_1 + 2r_1g_2 - 2s_1g_3 + 2r_2g_4$$

$$- 2s_2g_5 + \sum_{n=6}^{\infty}\begin{pmatrix} \ell r_i \\ \text{or} \\ \ell s_i \end{pmatrix} g_n$$

$$= \sum_{n=1}^{\infty} b_n G_n + \sum_{n=1}^{\infty} c_n g_n$$

where $c_n = \ell r_i$ or ℓs_i

$$b_n = kp_i \quad \text{or} \quad kq_i$$

and k, ℓ are certain real numbers.

The first five terms of b_i and c_i are

$b_1 = 2p_1$, $b_2 = 2p_2$, $b_3 = -q_2$, $b_4 = 2p_3$, $b_5 = -4q_3$, and

$c_1 = 2r_o$, $c_2 = 2r_1$, $c_3 = -2s_1$, $C_4 = 2r_2$, $c_5 = -2s_2$.

2.2 Derivation of the Functions g_i and G_i by Polynomial Method

The functions g_i and G_i can also be obtained by using a doubly infinite power series.

Suppose w_h is regular in the origin, then w_h can be written as the following doubly infinite series.

$$w_h = \sum_{m=0}^{\infty} \sum_{n=0}^{\infty} a_{mn} x^m y^n .$$

It is noted that the coefficients a_{mn} are not all linearly independent. The relationships among the coefficients a_{mn} can be found after satisfying the equation $\nabla^4 w_h = 0$.

Let $w_h = \sum_{m=0}^{p} \sum_{n=0}^{p} a_{mn} x^m y^n$, where $m + n \leq p$ and $p \geq 4$.

There are $[(p + 1)(p + 2)/2]$ coefficients of a_{mn}. Further the biharmonic equation $\nabla^4 w_h = 0$ gives rise to $[(p-3)(p-2)/2]$ "constraint" equations which define the relationships among the coefficients a_{mn}. The total number of independent coefficients a_{mn} is

$$\frac{(p + 1)(p + 2)}{2} - \frac{(p - 3)(p - 2)}{2} = 4p - 2 \qquad (4A)$$

The equation (4A) is valid for $p \geq 4$ only. Finally, the general solution of the biharmonic equation can be written as;

$$w_h = \sum_{m=0}^{p} \sum_{n=0}^{p} a_{mn} x^m y^n = \sum_{j=1}^{(2p-3)} b_j G_j + \sum_{i=1}^{(2p+1)} c_i g_i \qquad (4B)$$

where $m + n \leq p$ and $p \leq 4$ and the coefficients b_i and c_i are now all linearly independent.

As $p \to \infty$, equation (4B) can be written as;

$$w_h = \sum_{m=0}^{\infty} \sum_{n=0}^{\infty} a_{mn} x^m y^n = \sum_{j=1}^{\infty} b_j G_j + \sum_{i=1}^{\infty} c_i g_i \qquad (4C)$$

For more details, see Appendix 2.

It is noted that the sequence $x^m y^n$, $\begin{matrix} m=0,1,2,3,... \\ n=0,1,2,3,... \end{matrix}$

is complete approximating basis for a continuous function $w(x, y)$ which is finite at the origin.

The functions G_i and g_i may be regarded as complete approximating basis for the general solution of the biharmonic equation provided the solution is regular in the origin.

A computer programme was written to obtain results using the point-matching technique. The Jordan reduction method was used to solve the simultaneous linear algebraic equations to obtain the coefficients b_i and c_i of the general solution G_i and g_i.

CHAPTER III

APPLICATIONS TO SMALL DEFLECTIONS OF LATERALLY LOADED PLATES WITH ALL EDGES CLAMPED

3.1 Uniformly Loaded Rectangular Plates with All Edges Clamped

The problem of bending of clamped rectangular plates under uniform loading has attracted many investigators in the past and various approximate methods of solution are available in the literature. The most notable is the well-known solution of Timoshenko [1] where the Levy solution for a uniformly loaded simply supported rectangular plate was employed and edge moments were applied in such a way that the resulting slopes on all four edges are approximately zero. This method of solution leads to a doubly infinite set of simultaneous equations. The improved method of solution by point-matching was discussed by Conway [2] and more recently by Lo and Niedenfuhr [9]. Due to the symmetry of the problem (see Fig. 1(a)), the general solution can be written as,

$$w = \frac{q}{D}\left[\frac{1}{64}(x^4 + x^2y^2 + y^4) + c_1g_1 + b_1G_1 + \sum_{k=1}^{N}(c_{4k}g_{4k} + b_{4k}G_{4k})\right] \quad (5)$$

The numerical results after satisfying the boundary conditions $w = 0$, $\frac{\partial w}{\partial x} = 0$ at 5 equally spaced points along the edge AB and $w = 0$, $\frac{\partial w}{\partial y} = 0$ at 4 equally spaced points along the edge BC are shown in Table 1 and compared with the results from Timoshenko and Woinowsky-Krieger [1]. It is seen that the results from the present analysis are very

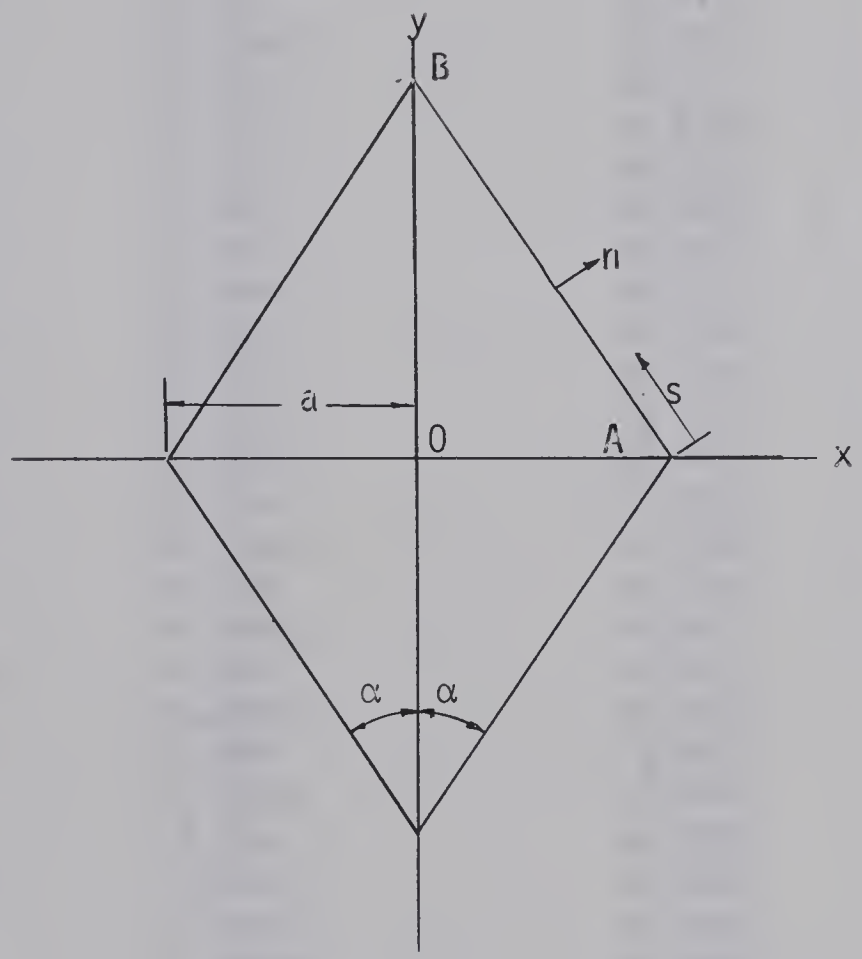

(b) Rhombus Plate

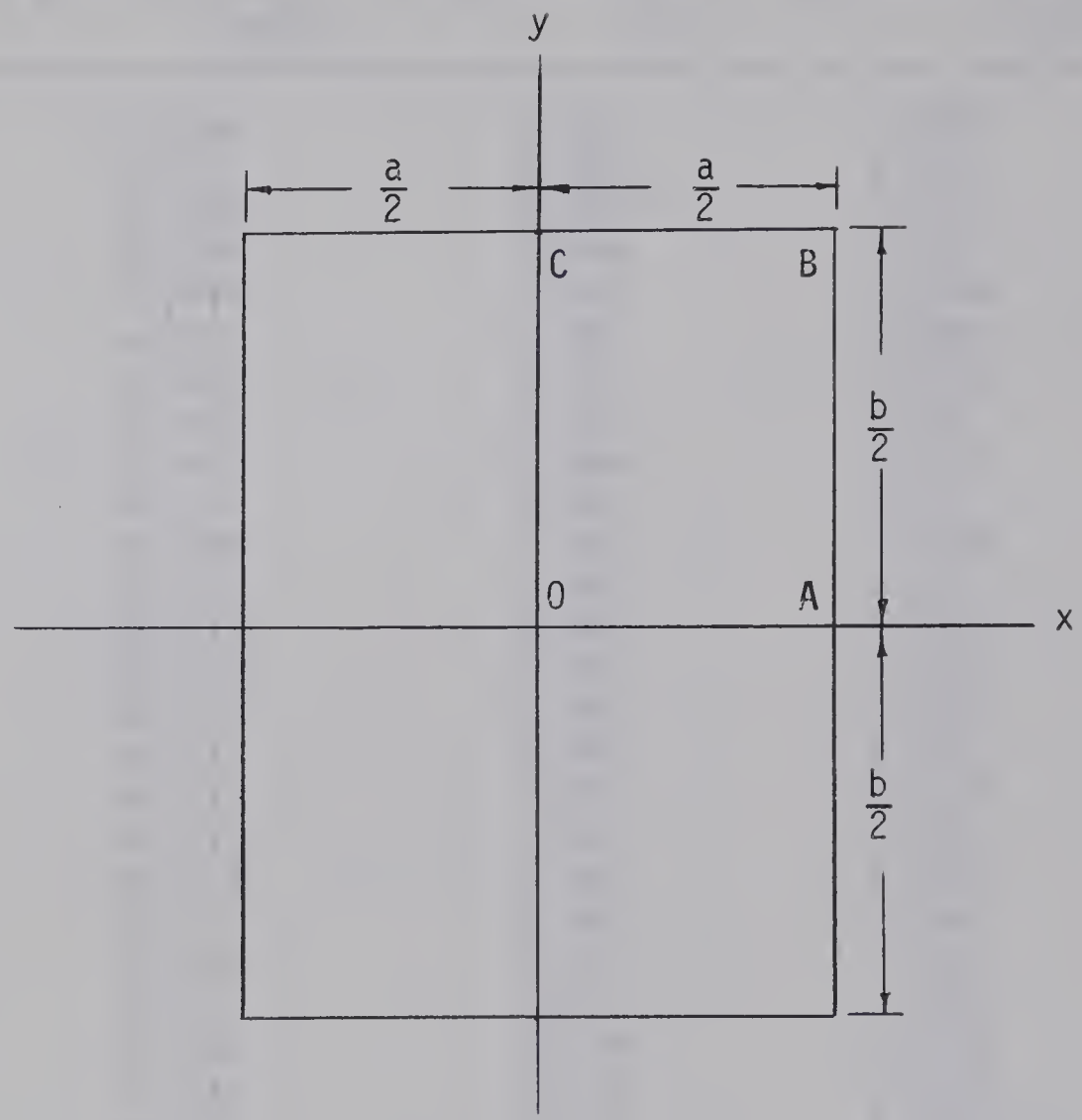

(a) Rectangular Plate

Fig. 1 Coordinate systems

Table 1 Deflections and Bending Moments for a Uniformly Loaded Rectangular Plate With All Edges Clamped, Poissons Ratio = 0.3

b/a	$(wx10^2/(qa^4/D))_{\substack{x=0\\y=0}}$	$(M_x x10/qa^2)_{\substack{x=a/2\\y=0}}$	$(M_y x10/qa^2)_{\substack{x=0\\y=b/2}}$	$(M_x x10/qa^2)_{\substack{x=0\\y=0}}$	$(M_y x10/qa^2)_{\substack{x=0\\y=0}}$
1.0	0.1265	-0.5134	-0.5134	0.2290	0.2290
	0.126	-0.513	-0.513	0.231	0.231
1.1	0.1508	-0.5813	-0.5386	0.2669	0.2315
	0.150	-0.581	-0.538	0.264	0.231
1.2	0.1725	-0.6396	-0.5544	0.2997	0.2284
	0.172	-0.639	-0.554	0.299	0.228
1.3	0.1912	-0.6880	-0.5636	0.3273	0.2216
	0.191	-0.687	-0.563	0.327	0.222
1.4	0.2069	-0.7271	-0.5685	0.3498	0.2126
	0.207	-0.726	-0.568	0.349	0.212
1.5	0.2197	-0.7579	-0.5709	0.3678	0.2026
	0.220	-0.757	-0.570	0.368	0.203
1.6	0.2300	-0.7817	-0.5717	0.3818	0.1925
	0.230	-0.780	-0.571	0.381	0.193
1.7	0.2382	-0.7998	-0.5718	0.3927	0.1826
	0.238	-0.799	-0.571	0.392	0.182
1.8	0.2446	-0.8133	-0.5716	0.4010	0.1735
	0.245	-0.812	-0.571	0.401	0.174
1.9	0.2496	-0.8231	-0.5712	0.4071	0.1653
	0.249	-0.822	-0.571	0.407	0.165
2.0	0.2533	-0.8301	-0.5709	0.4115	0.1581
	0.254	-0.829	-0.571	0.412	0.158
3.0	0.2617	-0.8391	-0.5703	0.4190	0.1269
4.0	0.2607	-0.8350	-0.5716	0.4170	0.1246
5.0	0.2604	-0.8340	-0.5787	0.4165	0.1245
6.0	0.2603	-0.8333	-0.5962	0.4163	0.1242
7.0	0.2600	-0.8326	-0.6268	0.4158	0.1237
∞	0.260	-0.833	-0.571	0.417	0.125

Note: The numerical results with 4 figures represent present analysis and the ones with 3 figures are from Timoshenko and Woinowsky-Krieger [1].

satisfactory. Incidentally, independent calculation shows that the value 0.0231 given for $(M_x)_{x=0,y=0}$ and $(M_y)_{x=0,y=0}$ with $\frac{b}{a} = 1.0$ in Timoshenko and Woinowsky-Krieger's book [1] is slightly in error and the correct value is 0.0229.

The boundary errors for deflection and slope are less than 1.6% and 3.8%, respectively, of the maximum values of the deflection and slope inside the plate when $\frac{b}{a} \leq 3$. In general, the boundary errors increase as the ratio $\frac{b}{a}$ increases. It is noted that forms of particular solutions such as $w_p = \frac{q}{48D}(x^4 + y^4)$ and $w_p = \frac{q}{8D}(x^2y^2)$ may be used and they all lead to the same results. In actual computation, it is more convenient to use

$$w_p = \frac{q}{64D}(x^4 + 2x^2y^2 + y^4).$$

3.2 Uniformly Loaded Clamped Rhombus Plates

The symmetry of the problem (see Fig. 1(b)) shows that the equation (5) can also be used for the rhombus plate with all edges clamped. The numerical results after satisfying the boundary conditions $w = 0$, $\frac{\partial w}{\partial n} = 0$ at 9 equally spaced points along the edge AB are listed in Table 2 together with the available results from the literature [1,10,11]. The agreement among the various results is good except in the case $\alpha = 10°$ where a maximum error of about 3% was observed for the maximum deflection.

The edge bending moment distribution are shown in Fig. 2. For the angle $\alpha \leq 20°$, some irregularities exist around the acute corner. This

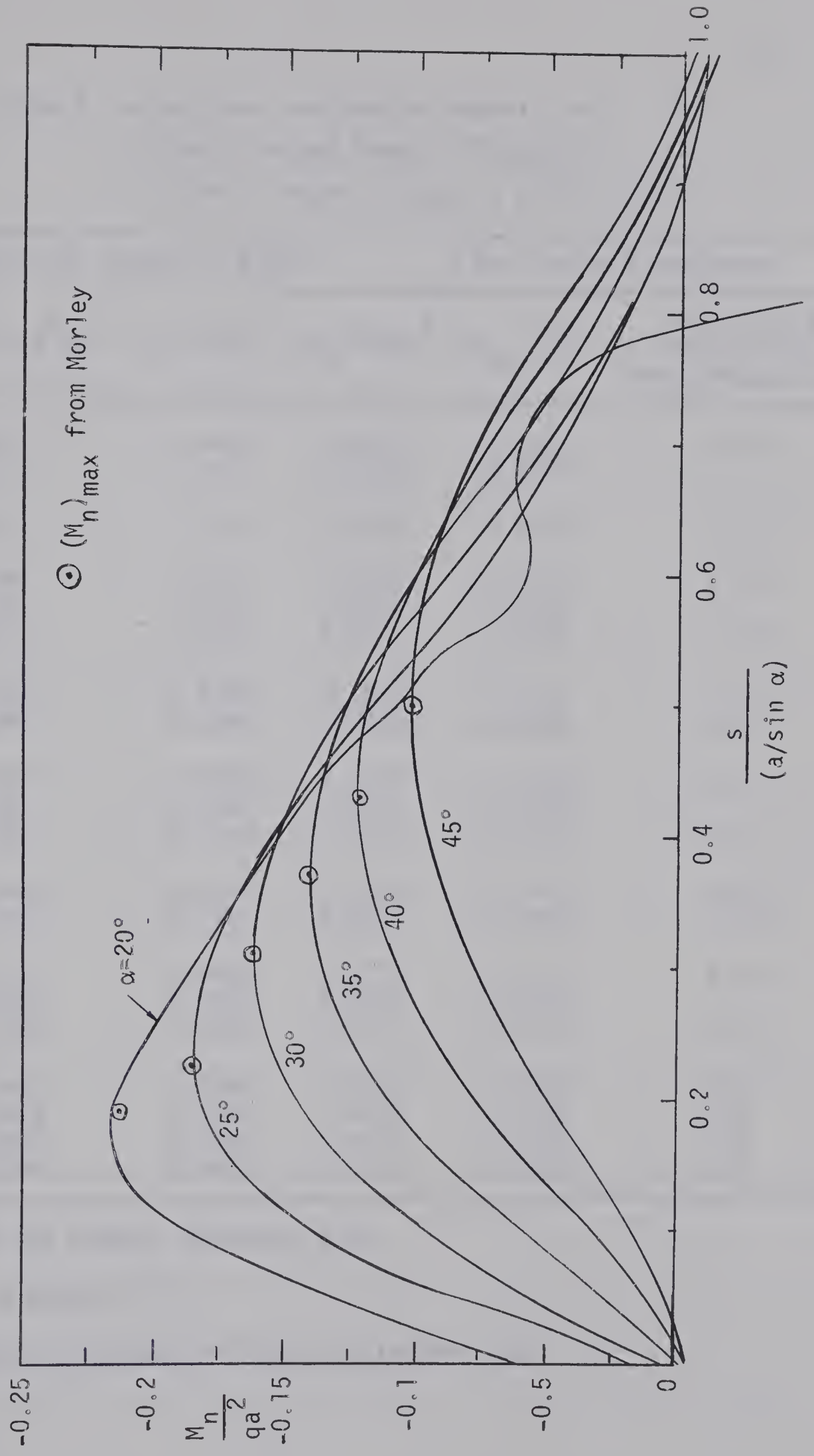

Fig. 2 Distribution of the bending moment M_n along the edge

Table 2 Deflections and Bending Moments for a Uniformly Loaded Rhombus Plate With All Edges Clamped, Poisson's Ratio = 0.3

α degrees	Values at center of plate: $wx10^2/(qa^4/D)$	$M_x x10/qa^2$	$M_y x10/qa^2$	Max. value along edge: M_{max}/qa^2	At distance $s/(a/\sin\alpha)$ from obtuse corner
10	3.021	1.359	0.6921	-0.2677	0.14
(1)*	2.819	1.347	0.7200	-0.2787	--
15	2.436	1.198	0.6906	-0.2499	0.16
20	1.964	1.054	0.6766	-0.2175	0.18
(1)	1.961	1.055	0.6746	-0.2095	--
(2)*	1.974	1.056	0.6771	-0.2120	0.18
25	1.567	0.9190	0.6527	-0.1847	0.22
(2)	1.568	0.9188	0.6528	-0.1859	0.22
30	1.229	0.7914	0.6172	-0.1620	0.31
(1)	1.230	0.7916	0.6176	-0.1624	--
(2)	1.230	0.7916	0.6176	-0.1628	0.31
35	0.9432	0.6718	0.5715	-0.1410	0.36
(2)	0.9433	0.6717	0.5714	-0.1410	0.37
40	0.7031	0.5606	0.5177	-0.1211	0.43
(1)	0.7032	0.5607	0.5177	-0.1210	--
(2)	0.7029	0.5605	0.5177	-0.1212	0.43
45	0.5061	0.4580	0.4580	-0.1026	0.5
(1)	0.5063	0.4582	0.4582	-0.1026	0.5
(2)	0.5040	0.4588	0.4578	-0.1024	0.5
(3)*	0.5040	0.4620	0.4620	-0.1026	0.5

* (1) Sattinger and Conway, Reference [10].

(2) Morley, Reference [11].

(3) Timoshenko and Woinowsky-Krieger, Reference [1].

phenomenon was also reported by Morley [11]. The boundary errors for the deflection and slope are less than 1.3% and 2%, respectively, of the maximum values of the deflection and slope inside the plate for $\alpha \geq 30°$. As the angle α decreases from 25° to 10°, the boundary errors around the acute corner gradually increase. Despite this difficulty in the vicinity of the acute corner for small angles α, the computed numerical results for the central deflections, bending moments and maximum edge moments are found to be very accurate compared with the results obtained by Morley [11] and Conway [10]. The bending moments M_x and M_y and the deflection computed at the plate corner are plotted in Fig. 3.

The numerical results after satisfying the boundary conditions $w = 0$ and $\frac{\partial w}{\partial n}$ at 8 and 10 equally spaced points along the edge AB are listed in Table 3 together with the results obtained by 9 points matched along edge AB. The results of Table 3 indicate the convergence of the solution.

3.3 Uniformly Loaded Circular Segmental Plates with All Sides Clamped

Bending of the uniformly loaded circular segmental plates with all edges clamped have been solved by Woinowsky-Krieger [12] using the bipolar coordinate transformation method. An alternate approach to solve this problem using point-matching was attempted. The symmetry of the problem (see Fig. 4) shows that a suitable general solution is

$$w = \frac{q}{D}\left[\frac{1}{64}(x^4 + 2x^2y^2 + y^4) + c_1g_1 + b_1G_1\right.$$

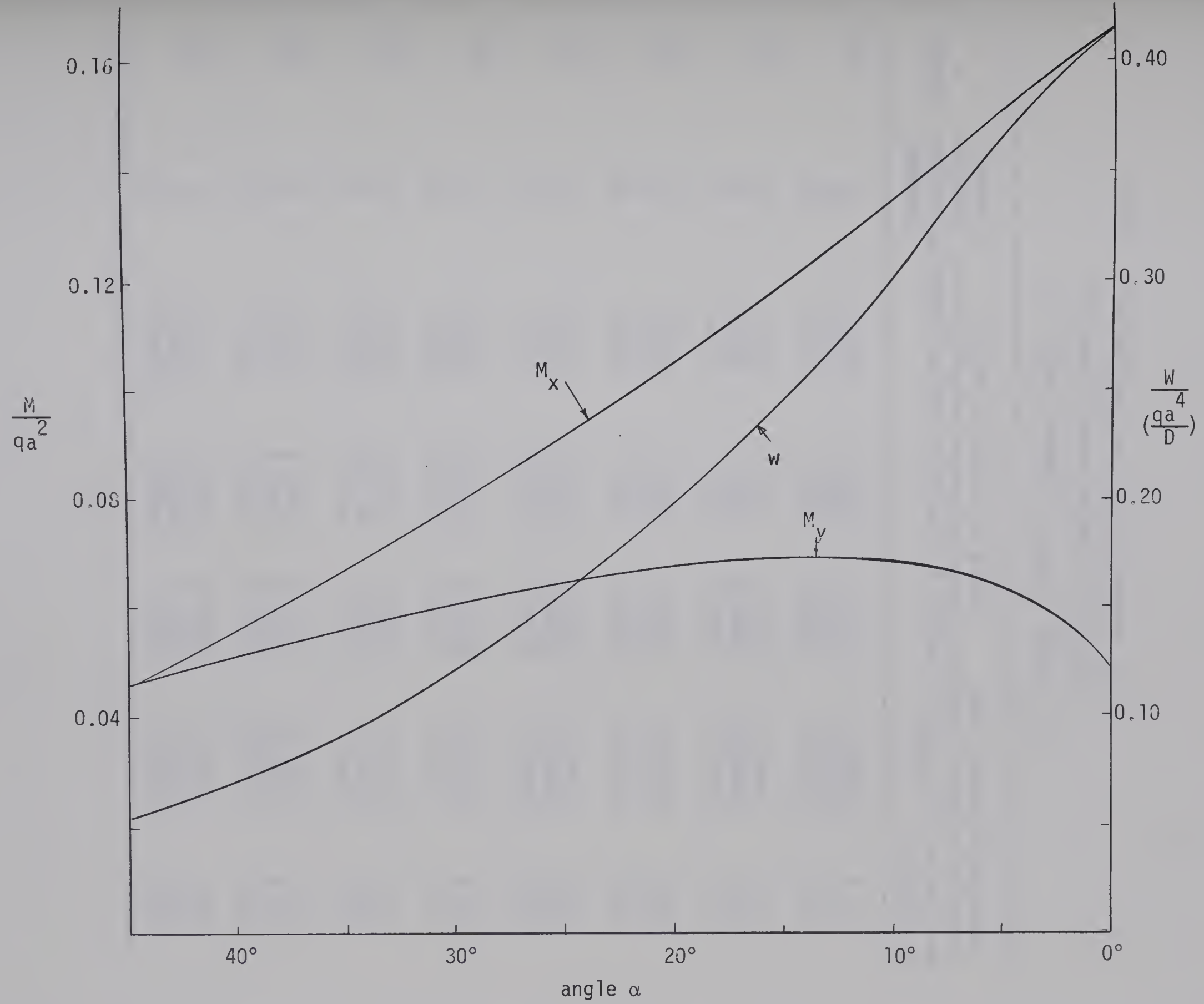

Fig. 3 Central deflections and bending moments for rhombus plates

Table 3 Deflections and Bending Moments for a Uniformly Loaded Rhombus Plate With All Edges Clamped, Poisson's Ratio = 0.3

α degrees	Number of points matched on boundary	Values at center of plate			Max. values along edge	
		$wx10^2/(qa^4/D)$	$M_x x10/qa^2$	$M_y x10/qa^2$	$(M_n)_{max}/qa^2$	at distance $s/(a/\sin\alpha)$
10°	8	3.0629	1.3682	0.70141	-0.26005	0.15
	9	3.0213	1.3596	0.69212	-0.26772	0.14
	10	2.9949	1.3552	0.68427	-0.27265	0.13
15°	8	2.4495	1.1981	0.69819	-0.24846	0.18
	9	2.4356	1.1980	0.69061	-0.24992	0.16
	10	2.4278	1.1982	0.68609	-0.24996	0.15
20°	8	1.9665	1.0536	0.67879	-0.21999	0.19
	9	1.9638	1.0543	0.67662	-0.21757	0.18
	10	1.9623	1.0547	0.67565	-0.21455	0.16
25°	8	1.5673	0.91887	0.65266	-0.18694	0.22
	9	1.5673	0.91906	0.65270	-0.18465	0.22
	10	1.5676	0.91915	0.65276	-0.18382	0.23
30°	8	1.2295	0.79147	0.61703	-0.16175	0.31
	9	1.2298	0.79145	0.61728	-0.16203	0.31
	10	1.2300	0.79145	0.61742	-0.16217	0.31
35°	8	0.94316	0.67191	0.57144	-0.14129	0.36
	9	0.94326	0.67187	0.57153	-0.14097	0.36
	10	0.94331	0.67185	0.57156	-0.14081	0.37
40°	8	0.70317	0.56066	0.51769	-0.12111	0.43
	9	0.70316	0.56065	0.51769	-0.12111	0.43
	10	0.70316	0.56065	0.51769	-0.12118	0.43
45°	8	0.50613	0.45809	0.45809	-0.10261	0.50
	9	0.506127	0.45809	0.45809	-0.10261	0.50
	10	0.506125	0.45809	0.45809	-0.10266	0.50

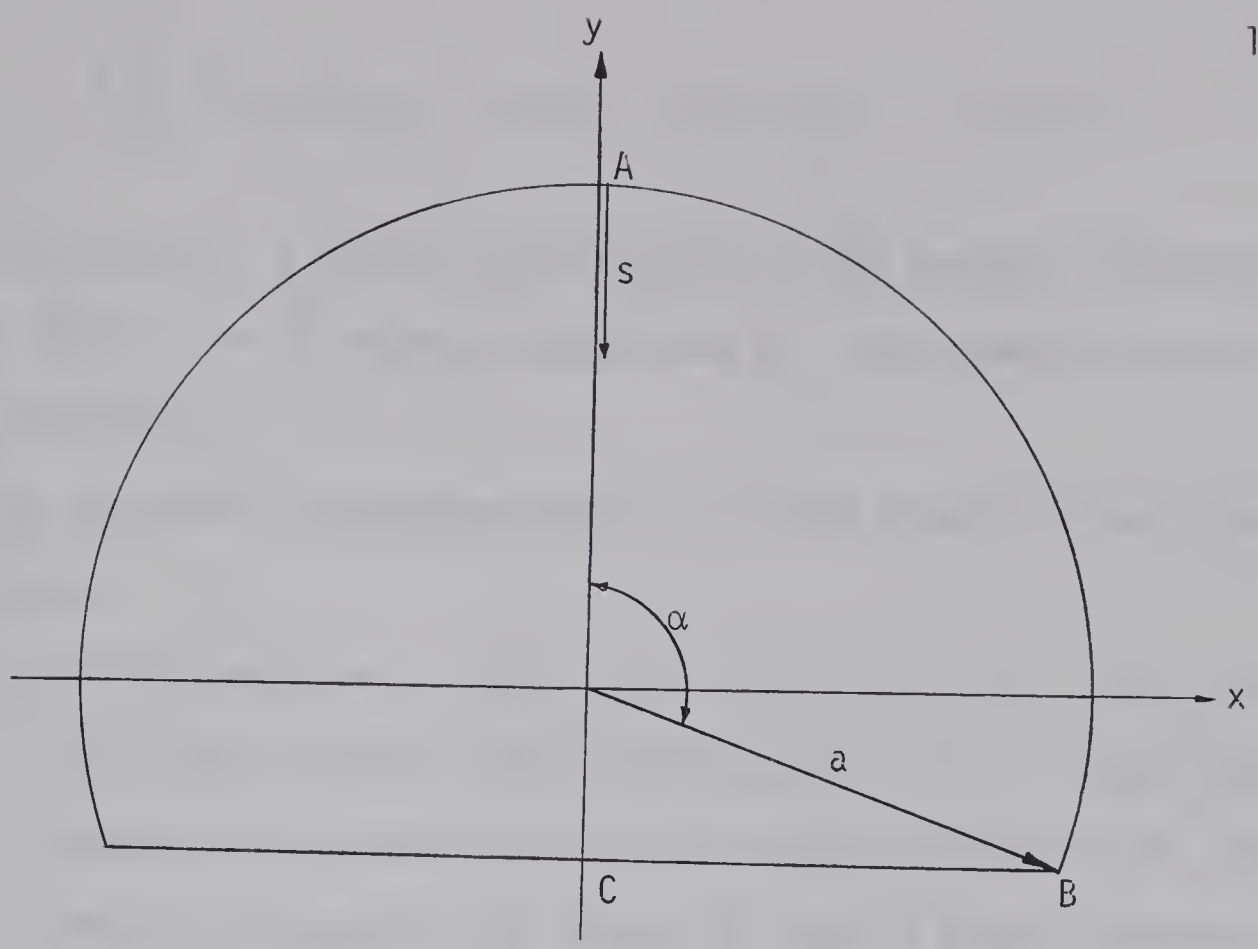

(a) $\alpha \geq \frac{\pi}{2}$

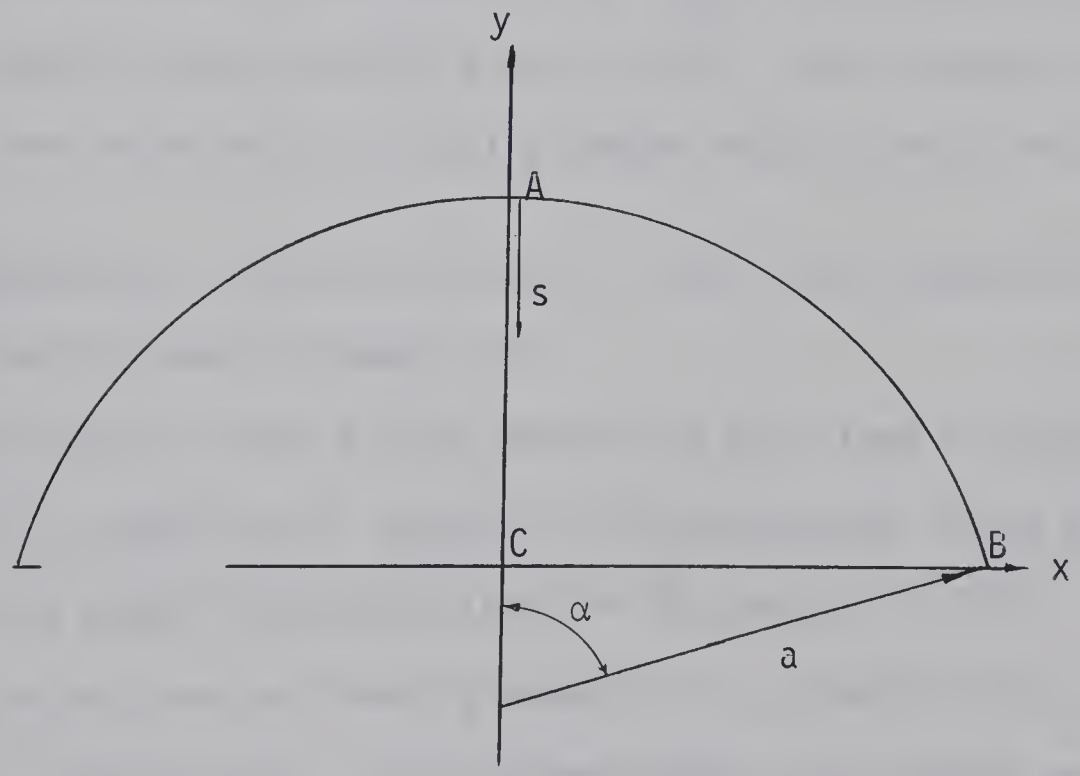

(b) $\alpha < \frac{\pi}{2}$

Fig. 4 Coordinate system for circular segmental plate

$$+ \sum_{k=1}^{N} (c_{4k-1}g_{4k-1} + c_{4k}g_{4k} + b_{4k-1}G_{4k-1} + b_{4k}G_{4k})] \qquad (6)$$

Selecting N = 9 permits satisfaction of the boundary conditions $w = 0$, $\frac{\partial w}{\partial n} = 0$ at 19 points along AB and BC. The numerical results are shown in Table 4.

The locations of matching points along the boundaries are chosen as follows:

a) In the cases of α = 180°, 170°, 160°, 150°, 140°, 130°, 120°, 110°, 100° and 90°, the matching points are so located that there is one point for every ten degrees along arc AB. The rest of the points are located at equally spaced intervals along line BC.

b) In the cases of α = 80°, 70°, 60°, 50°, 40°, 30°, 20° and 10°, the boundary conditions $w = 0$, $\frac{\partial w}{\partial n} = 0$ are satisfied at 10 equally spaced points along arc AB. These boundary conditions are satisfied at 9 equally spaced points along line BC.

The numerical results are shown in Table 4 and compared to the results from Woinowsky-Krieger [12].

The boundary errors for the deflection and slope are less than 0.1% and 1%, respectively, compared with the maximum values of the deflection and slope inside the plate for the angles $\alpha \geq 20°$.

The deflections and bending moments are plotted in Fig. 5, Fig. 6 and Fig. 7, respectively. The maximum moments for various angles α are also plotted in Fig. 8 where the dimensionless quantity is $[M_{max}/q(\overline{AC})^2]$. It is noted that the reference length AC is used rather

Table 4 Maximum Deflections and Bending Moments for a Uniformly Loaded Circular Segmental Plate With All Edges Clamped, Poisson's Ratio = 0.3.

	Maximum deflections		$(M_y)_{max}$ at point C, M_{max}/qa^2	
α degree	$w_{max}/(qa^4/D)$	at distance s/AC	This Work	Woinowsky-Krieger
10°	0.1383×10^{-9}	0.50	-0.1921×10^{-4}	-0.192×10^{-4}
20°	0.3409×10^{-7}	0.50	-0.3018×10^{-3}	-0.301×10^{-3}
30°	0.8191×10^{-6}	0.50	-0.1481×10^{-2}	-0.148×10^{-2}
40°	0.7469×10^{-5}	0.50	-0.4475×10^{-2}	-0.447×10^{-2}
50°	0.3949×10^{-4}	0.50	-0.1029×10^{-1}	-0.103×10^{-1}
60°	0.1465×10^{-3}	0.50	-0.1983×10^{-1}	-0.198×10^{-1}
70°	0.4217×10^{-3}	0.50	-0.3361×10^{-1}	-0.337×10^{-1}
80°	0.9893×10^{-3}	0.50	-0.5161×10^{-1}	-0.519×10^{-1}
90°	0.2022×10^{-2}	0.52	-0.7314×10^{-1}	-0.731×10^{-1}
100°	0.3582×10^{-2}	0.52	-0.9675×10^{-1}	-0.964×10^{-1}
110°	0.5626×10^{-2}	0.52	-0.1205	-0.123
120°	0.8113×10^{-2}	0.52	-0.1426	-0.146
130°	0.1065×10^{-1}	0.52	-0.1596	-0.161
140°	0.1290×10^{-1}	0.52	-0.1659	-0.171
150°	0.1440×10^{-1}	0.52	-0.1716	-0.178
160°	0.1526×10^{-1}	0.50	-0.1767	-0.170
170°	0.1559×10^{-1}	0.50	-0.1582	-0.154
180°	0.1562×10^{-1}	0.50	-0.1250	-0.125

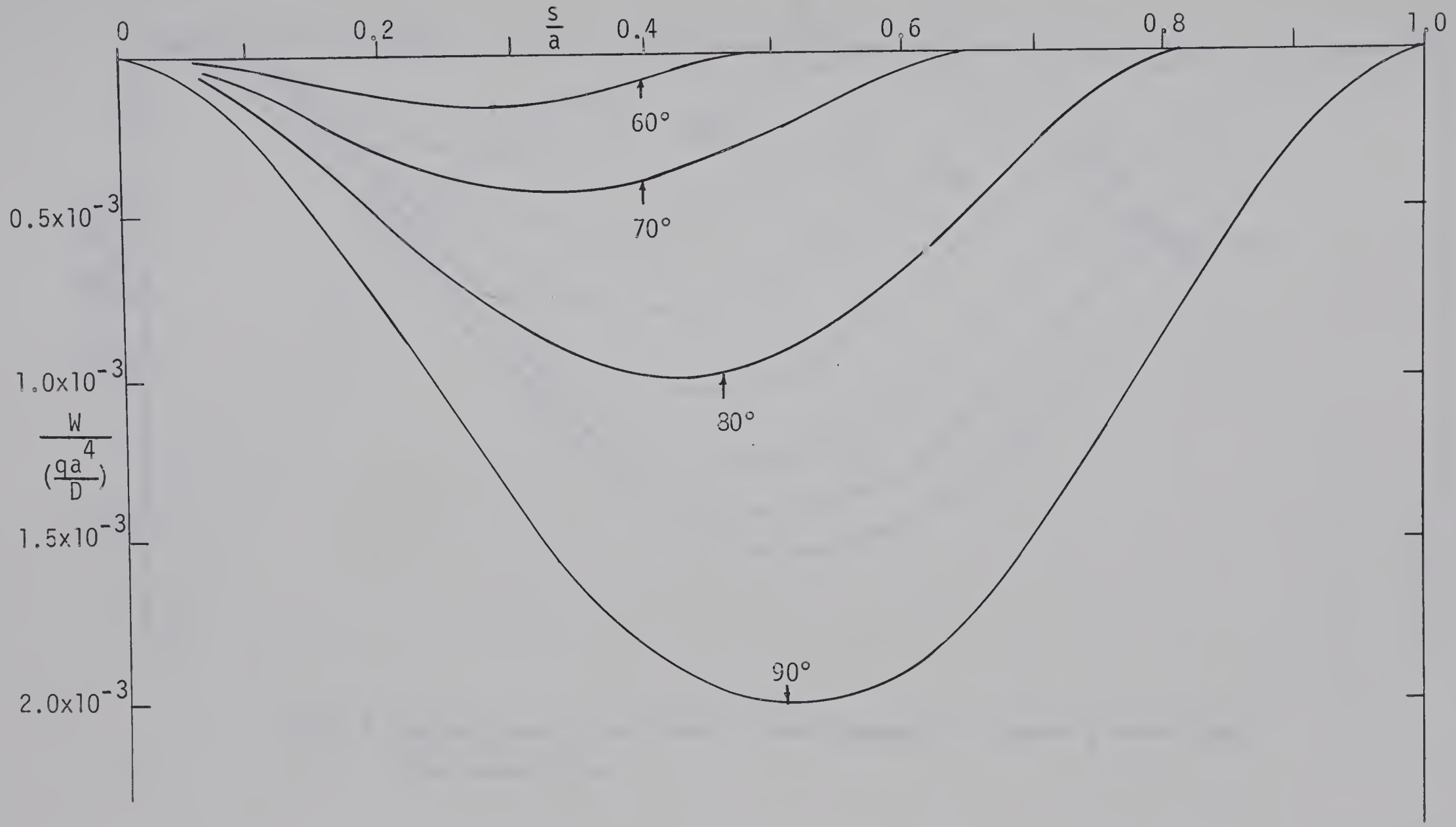

Fig. 5 Deflections of uniformly loaded segmental clamped plates along the center line

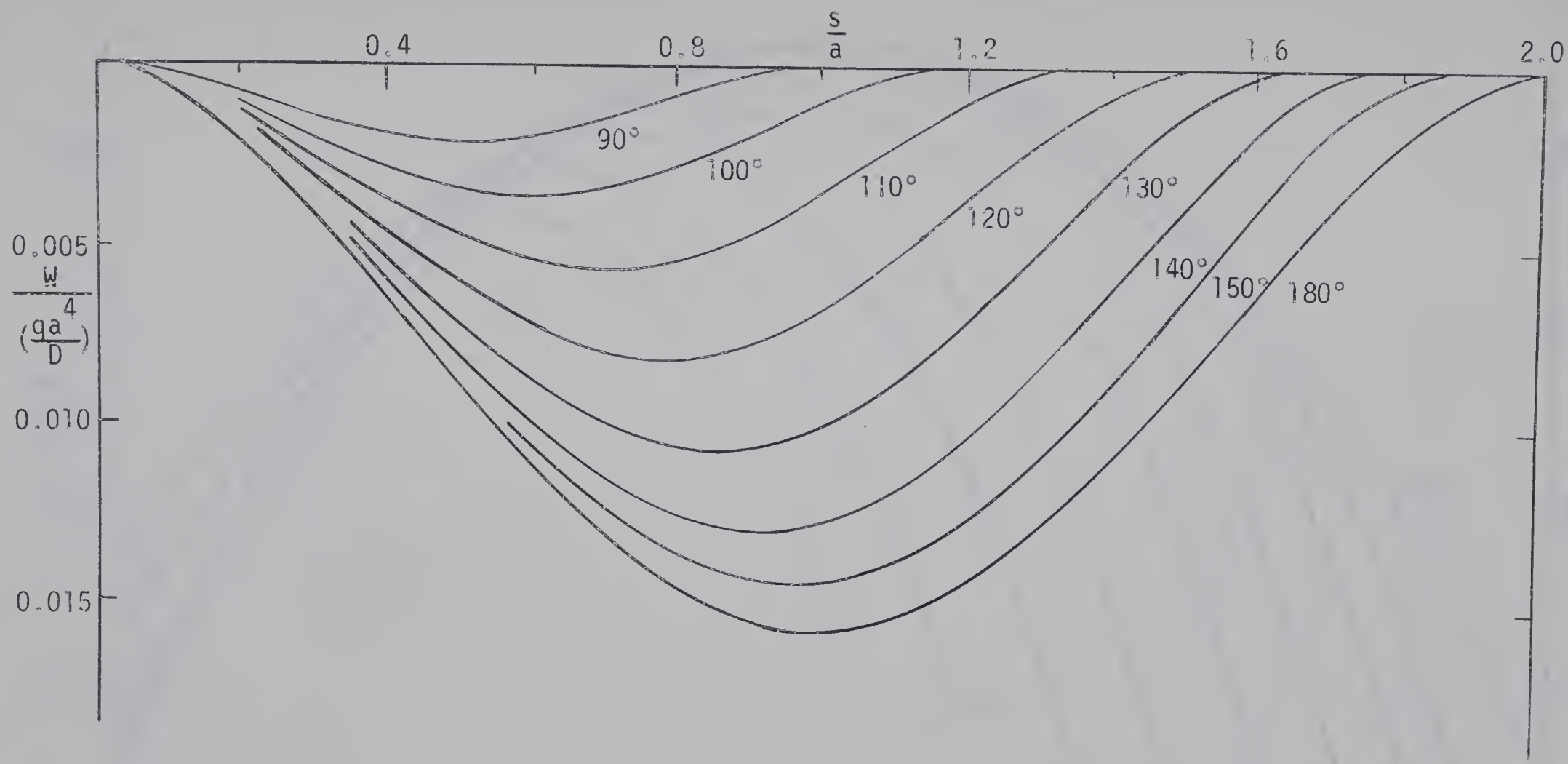

Fig. 6 Deflections of uniformly loaded segmental clamped plates along the center line

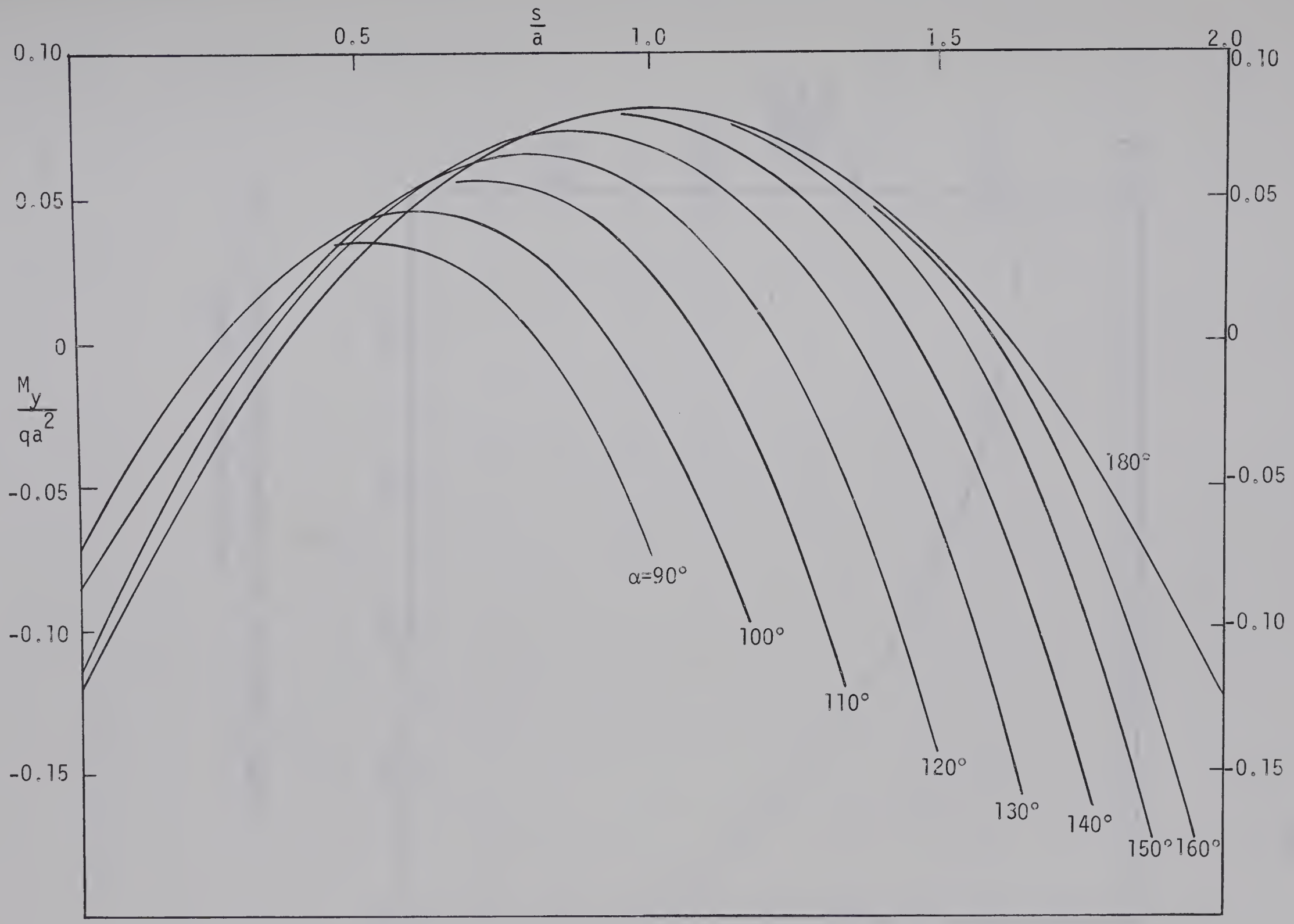

Fig. 7 Bending moment of uniformly loaded segmental clamped plates, along the center line

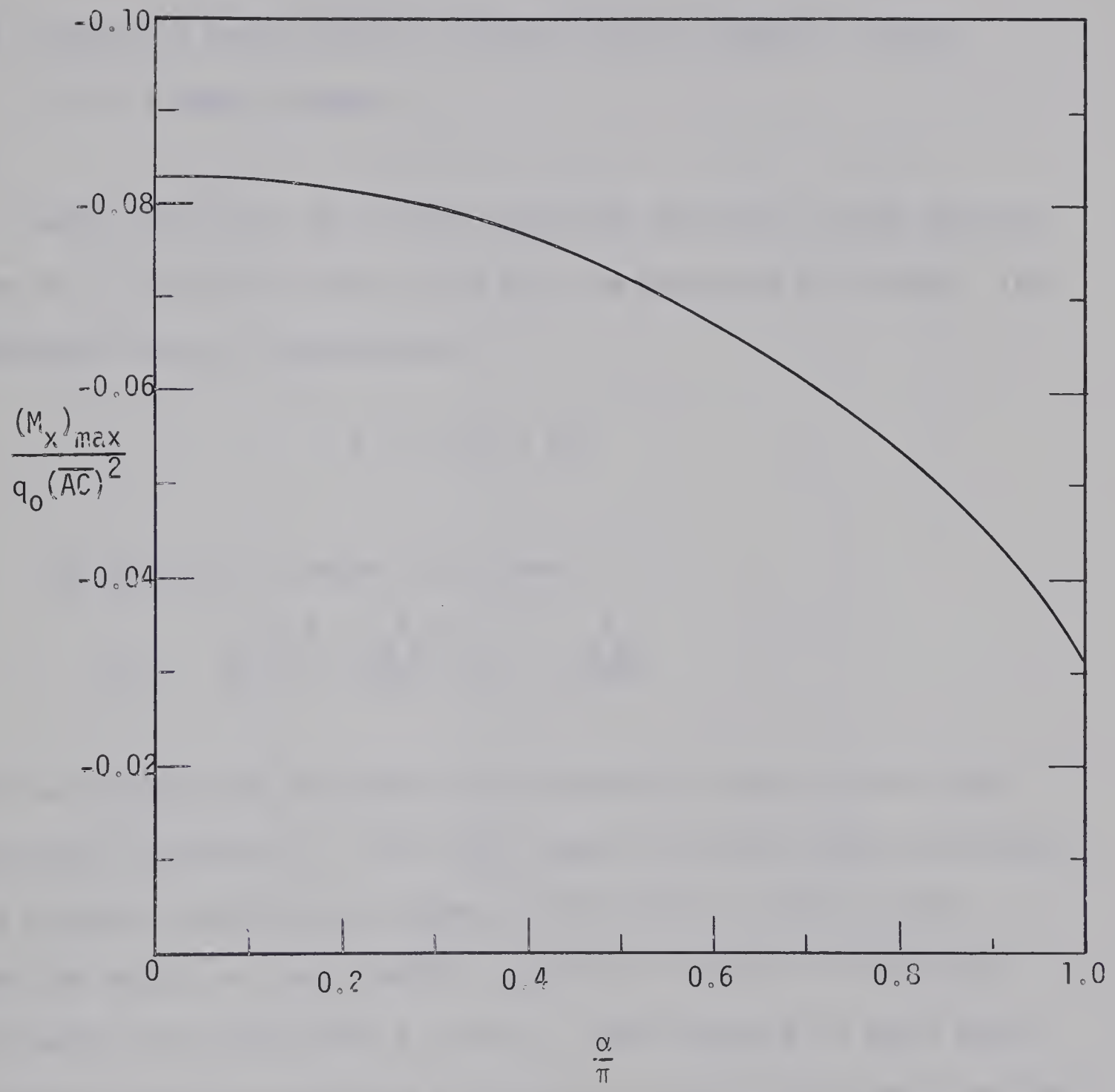

Fig. 8 Maximum bending moments for uniformly loaded segmental clamped plates

than the radius a.

3.4 Bending of Hydrostatically Loaded Circular Segmental Plates with All Edges Clamped

Referring to Fig. 9, all the conditions for this problem are the same as in the above section (3.3) with the exception of loading. The hydrostatic load is expressed as;

$$q = q_o(1 - \frac{y}{a}) .$$

The particular integral to be used is

$$w_p = \frac{q_o}{D} (\frac{x^4 + 2x^2y^2 + y^4}{64} - \frac{x^4y}{a24}) .$$

All the analyses are the same as the uniformly loaded circular plate discussed in section 3.3. The final numerical results after satisfying the boundary conditions are shown in Table 5 for α = 40° to 180°. When the angles are less than 40°, there are numerical difficulties in finding the coefficients b_i and c_i. Since plates with small angle α are not usually encountered in practice, so this limitation is not believed to be serious. The numerical results for this problem is believed to be new.

The boundary errors for the deflection and slope, respectively, are less than 1.0% and 3.4% of the maximum values of the deflection and slope inside the plate when the angles are $\alpha \geq 40°$.

Table 5 Maximum Deflections and Bending Moments for a Hydrostatically Loaded Circular Segmental Plate With All Edges Clamped, Poisson's Ratio = 0.3

α degrees	Maximum Deflection		$(M_y)_{max.}$ at point C
	$w_{max}/(q_o a^4/D)$	at distance S/AC	$(M_{max.})/(q_o a^2)$
40°	$0.8822 \cdot 10^{-6}$	0.52	$-0.6318 \cdot 10^{-3}$
50	$0.7083 \cdot 10^{-5}$	0.52	$-0.2221 \cdot 10^{-2}$
60°	$0.3778 \cdot 10^{-4}$	0.52	$-0.6055 \cdot 10^{-2}$
70°	$0.1435 \cdot 10^{-3}$	0.52	$-0.1357 \cdot 10^{-1}$
80°	$0.4317 \cdot 10^{-3}$	0.52	$-0.2640 \cdot 10^{-1}$
90°	$0.1063 \cdot 10^{-2}$	0.55	$-0.4559 \cdot 10^{-1}$
100°	$0.2213 \cdot 10^{-2}$	0.55	$-0.7126 \cdot 10^{-1}$
110°	$0.3999 \cdot 10^{-2}$	0.55	-0.1022
120°	$0.6431 \cdot 10^{-2}$	0.55	-0.1365
130°	$0.9267 \cdot 10^{-2}$	0.55	-0.1688
140°	$0.1202 \cdot 10^{-1}$	0.55	-0.1901
150°	$0.1406 \cdot 10^{-1}$	0.55	-0.2097
160°	$0.1531 \cdot 10^{-1}$	0.55	-0.2267
170°	$0.1578 \cdot 10^{-1}$	0.55	-0.2088
180°	$0.1582 \cdot 10^{-1}$	0.55	-0.1667

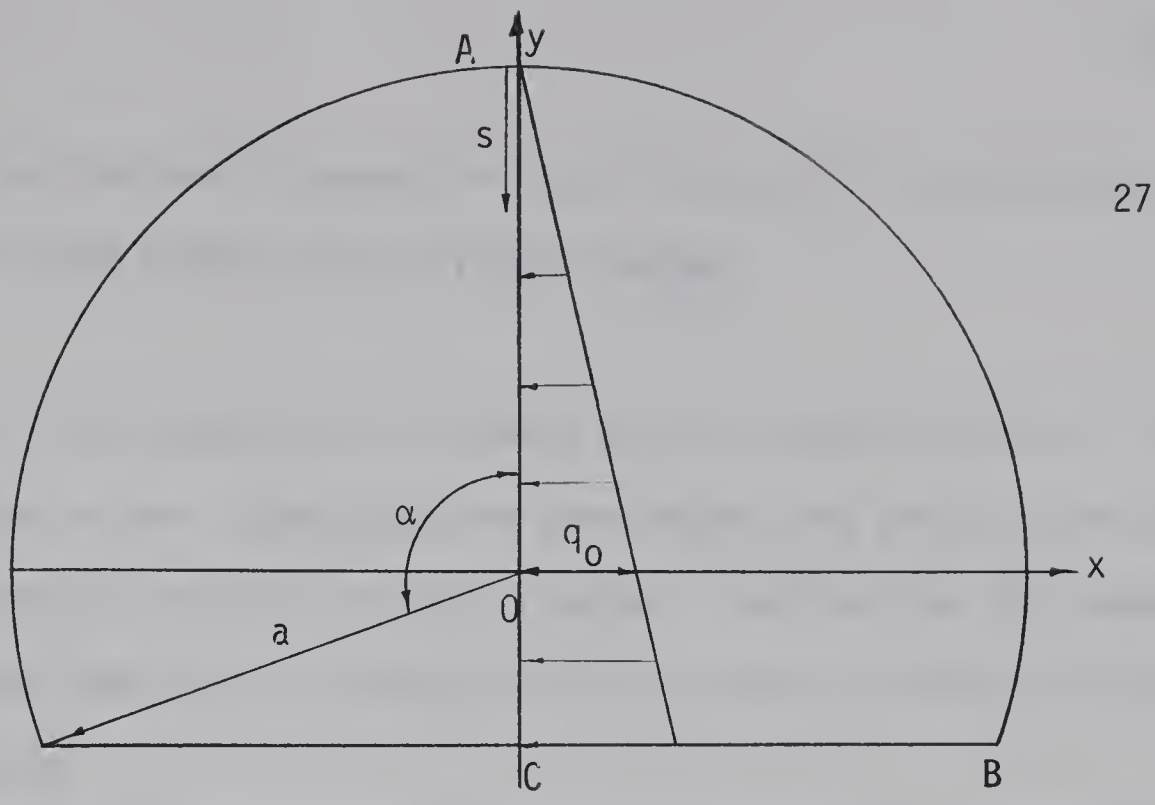

Fig. 9 Coordinate system for hydrostatically loaded circular segmental clamped plate

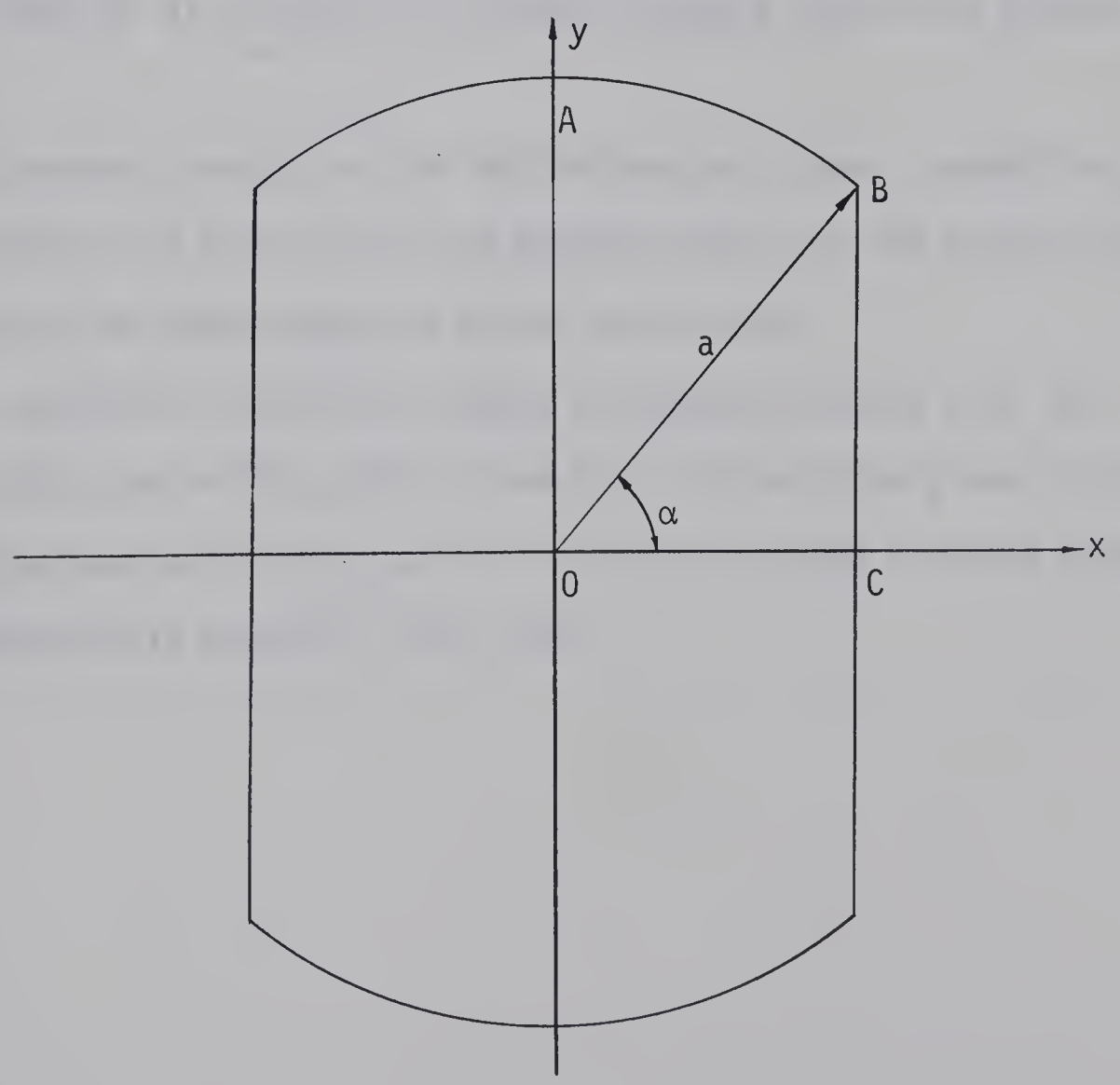

Fig. 10 Coordinate system for uniformly loaded circular plates with diametrically opposite flat sides

3.5 Bending of Uniformly Loaded Circular Plates with Diametrically Opposite Flat Sides with All Edges Clamped

Because of the practical importance and the unavailability of the exact solution in the literature, the same method and analysis are used to obtain numerical results for this problem. Considering the symmetry of the problem (see Fig. 10), equation (5) is also a suitable solution to this problem.

The numerical results after satisfying the boundary conditions $w = 0$, $\frac{\partial w}{\partial n} = 0$ along the circular arc AB and $w = 0$, $\frac{\partial w}{\partial x} = 0$ along straight edge BC at a total of 10 equally spaced points are listed in Table 6.

The boundary errors for the deflection and slope, respectively, are less than 0.1% and 0.3% of the maximum values of the deflection and slope inside the plate when the angles are $\alpha \leq 80°$.

The numerical results of clamped rectangular plates with the height, 2(AO), and width, 2(OC), (see Fig. 10) are also given in Table 6 for comparison with the results of uniformly loaded circular plates with diametrically opposite flat sides.

Table 6 Maximum Deflections and Bending Moments for a Uniformly Loaded Clamped Circular Plate With Diametrically Opposite Flat Sides

α	$\frac{w}{(\frac{qa^4}{D})}\Big\|_{\substack{x=0\\y=0}}$	$\frac{M_{max}}{qa^2}$ at C	$\frac{M_x}{qa^2}\Big\|_{\substack{x=0\\y=0}}$	Note
80°	0.3788×10^{-4} $*0.378 \times 10^{-4}$	-0.1005×10^{-1} $*-0.101 \times 10^{-1}$	0.5025×10^{-2} $*0.502 \times 10^{-2}$	$\frac{AO}{OC} = 5.76$
70°	0.5732×10^{-3} $*0.573 \times 10^{-3}$	-0.3923×10^{-1} $*-0.392 \times 10^{-1}$	0.1962×10^{-1} $*0.196 \times 10^{-1}$	$\frac{AO}{OC} = 2.924$
60°	0.2524×10^{-2} $*0.253 \times 10^{-2}$	-0.8271×10^{-1} $*-0.830 \times 10^{-1}$	0.4105×10^{-1} $*0.412 \times 10^{-1}$	$\frac{AO}{OC} = 2.0$
50°	0.6045×10^{-2} $*0.614 \times 10^{-2}$	-0.1257 $*-0.127$	0.6121×10^{-1} $*0.617 \times 10^{-1}$	$\frac{AO}{OC} = 1.556$
40°	0.1008×10^{-1}	-0.1547	0.7433×10^{-1}	
30°	0.1316×10^{-1}	-0.1683	0.7967×10^{-1}	
20°	0.1493×10^{-1}	-0.1637	0.8113×10^{-1}	
10°	0.1556×10^{-1}	-0.1542	0.8125×10^{-1}	
0°	0.15625×10^{-1}	-0.1250	0.8125×10^{-1}	

* Results from clamped rectangular plate with height 2(AO) and width 2(OC).

CHAPTER IV

APPLICATIONS TO CREEPING FLOW PROBLEMS IN SHALLOW CAVITIES WITH VARIOUS SHAPES

4.1 Introduction

The motion generated in a fluid-filled cavity by a uniform translation of one of the walls (see Figs. 11, 12 and 18) represents one of the simplest examples of the steady flow involving closed streamlines, and as such has occupied a position of considerable theoretical importance within the broader field of steady separated flows. Previous work on this topic has been reviewed by Burggraf [13], who, for the special case of square cavity, also obtained numerical solution to the full Navier-Stokes equation for a range of Reynolds number $R \equiv V_o D/\nu$ from 0 to 400 (V_o is the velocity of the top wall, D is the width of the cavity and ν is the kinematic viscosity of the fluid).

In the absence of the inertia terms, the equation of motion reduces to the familiar biharmonic equation $\nabla^4\psi = 0$, where ψ is the dimensionless stream function. The boundary conditions are:

$$\psi = 0 \qquad \text{on all boundaries,}$$

$$\frac{\partial\psi}{\partial y} = 1 \qquad \text{at the upper moving wall,}$$

and

$$\frac{\partial\psi}{\partial n} = 0 \qquad \text{at the fixed walls.}$$

Here, n is the outward normal. As already remarked by Burggraf [13], the form of the boundary conditions precludes an analytic solution of this system by one of the standard procedures used successfully in the

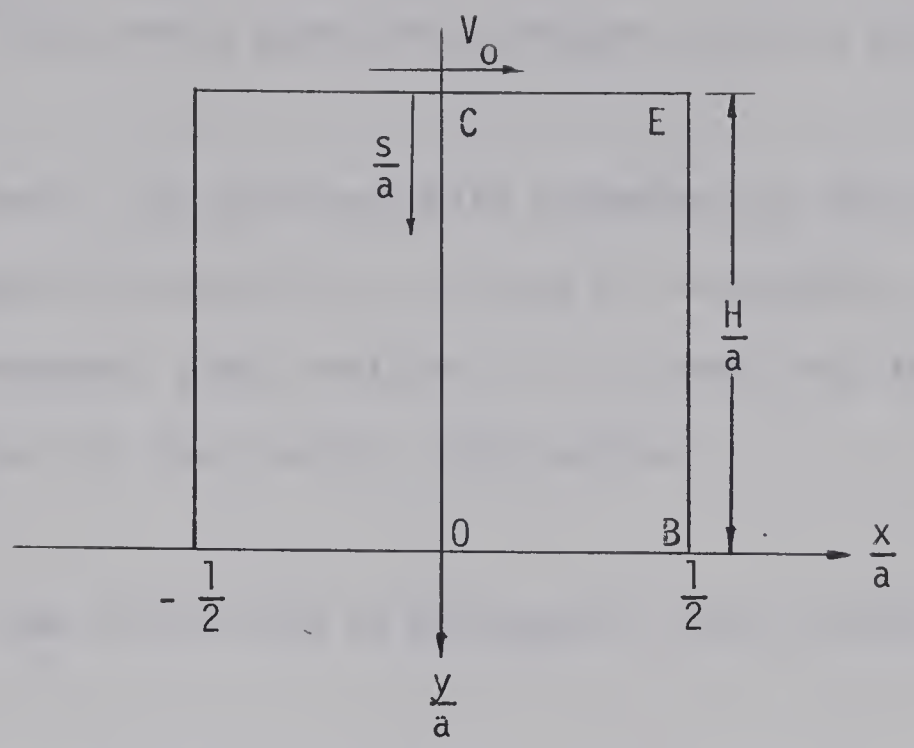

Fig. 11 Coordinate system for a rectangular cavity

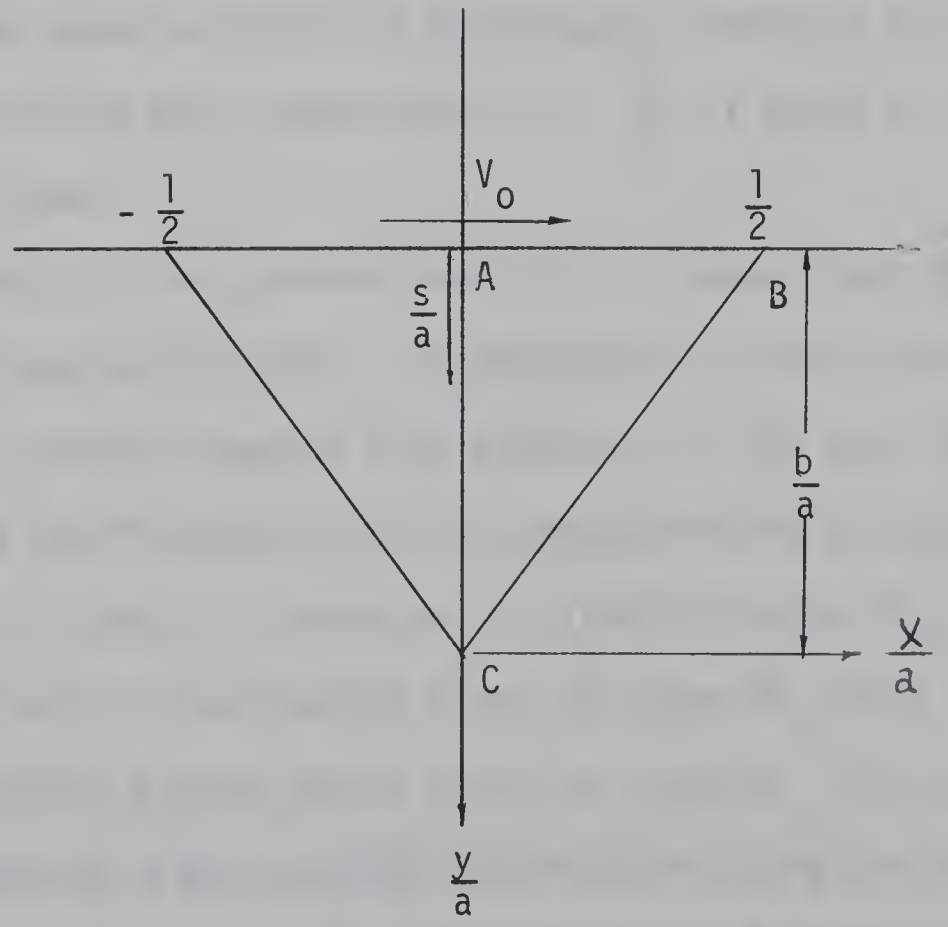

Fig. 12 Coordinate system for a triangular cavity

field of elasticity, or by approximate methods, such as variational technique.

In this thesis, the point-matching technique was applied to obtain approximate numerical results for cavities of rectangular, triangular and circular segmental cross sections. It is noted that the particular integral vanishes for the creeping flow problem.

4.2 Creeping Flow in Cavities of Rectangular Cross Section

Creeping flow solutions for rectangular cavities having aspect ratios, $A = \frac{H}{a} = \frac{1}{4}, \frac{1}{2}, 1, 2, 3$ and 5 were obtained numerically by a relaxation technique in 1966 by Pan and Acrivos [14]. In this thesis the general solution of biharmonic equation, g_i and G_i, in Cartesian coordinates was used to obtain an approximate numerical solution for rectangular cavities with aspect ratio $A = \frac{H}{a} = 1$ and 2 by the point-matching technique.

The symmetry of the problem (see Fig. 11) shows that equation (6) is a suitable general solution. As noted earlier, the particular integral vanishes for the creeping flow problem. In the case of aspect ratio, $A = \frac{H}{a} = 1$, the coefficients c_i and b_i are determined by satisfying $\psi = 0$ and $\frac{\partial \psi}{\partial y} = 1$ at 5 equally spaced points along the edge CE, $\psi = 0$ and $\frac{\partial \psi}{\partial y} = 0$ at 5 equally spaced points along the edge OB, and $\psi = 0$ and $\frac{\partial \psi}{\partial x} = 0$ at 9 equally spaced points along the edge BE. The numerical results of streamline ψ and velocity distribution along the center line are plotted in Fig. 13. In the case of the aspect ratio = 2, the numerical results after satisfying the boundary conditions $\psi = 0$ and $\frac{\partial \psi}{\partial y} = 1$

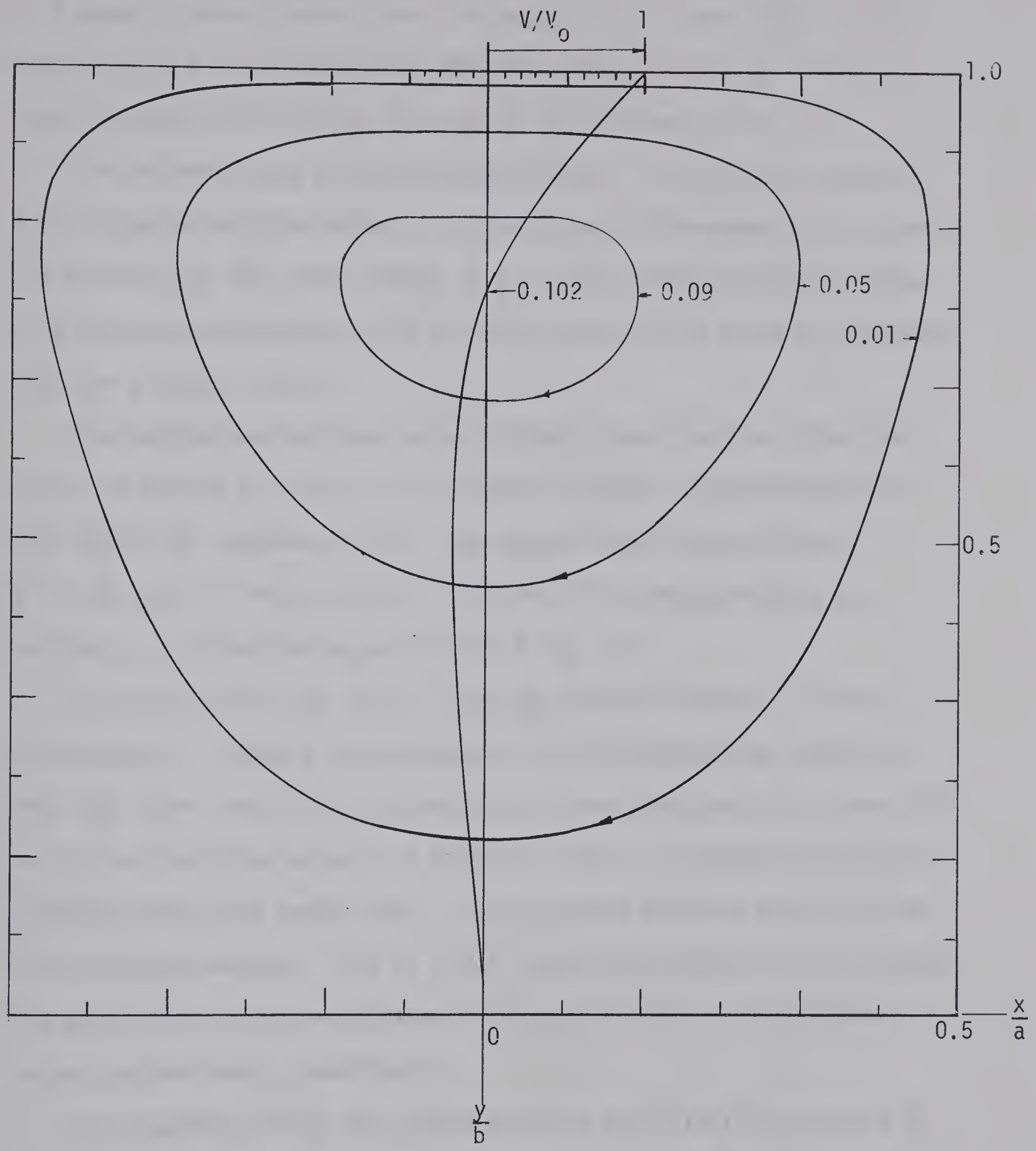

Fig. 13 Creeping flow streamline patterns and velocity distribution along the center line for square cavity

at 4 equally spaced points along the edge CE, $\psi = 0$ and $\frac{\partial \psi}{\partial y} = 0$ at 4 equally spaced points along the edge OB, and $\psi = 0$ and $\frac{\partial \psi}{\partial x} = 0$ at 11 equally spaced points along the edge BE are plotted in Fig. 14.

The maximum value of the stream function at the first vortex is 0.102 compared with the value 0.1 given by both references [13, 14] and the location of the vortex center is $\frac{s}{a} = 0.235$ compared with the value of 0.24 given by reference [14] and the value of 0.25 given by reference [13] for a square cavity.

The maximum and minimum values of the stream function ψ for the first and second vortices are 0.102 and -0.000249, respectively (0.1 and -0.00023 by reference [14]). The vortex center locations are $\frac{s}{a} = 0.26$ and 1.55 respectively, (0.25 and 1.575, respectively, by reference [14]) for the aspect ratio $A = \frac{H}{a} = 2$.

It is seen that the results from the present analysis are very satisfactory. The only disadvantage of the point-matching method is that the lower corner vortices which have been discussed by Acrivos [14] can not be predicted because of boundary errors. But the velocity distribution along the center line, Y axis, can be obtained easily by the point-matching method. This is a very important property of the problem. The numerical results are plotted in Fig. 13 and Fig. 14 for aspect ratios one and two, respectively.

The boundary errors for stream function and velocity expressed as a percentage of their maximum values are less than 0.6% and 4%, respectively, for the aspect ratio $A = \frac{H}{a} = 1$. The boundary errors for stream function and velocity expressed as a percentage of their maximum values are less than 1.0% and 5%, respectively, for the aspect ratio $A = \frac{H}{a} = 2$.

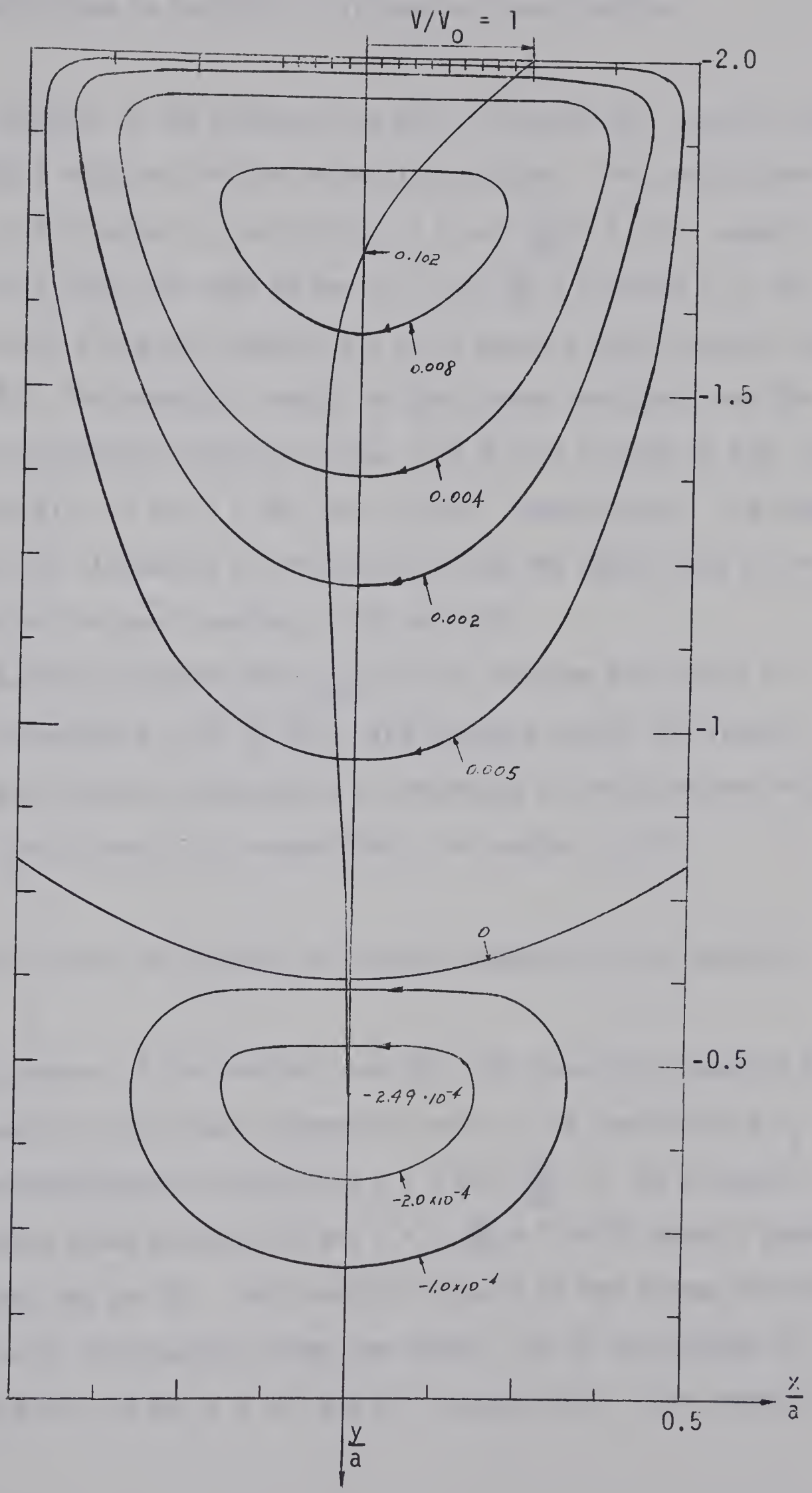

Fig. 14 Creeping flow streamline patterns and velocity distribution along the center line for rectangular cavity A = H/a = 2.

4.3 Creeping Flow in Cavities of Triangular Cross Section

The symmetry of the problem (see Fig. 12) shows that equation (6) is a suitable solution for the triangular cavities. The coefficients b_i and c_i are obtained by satisfying $\psi = 0$ and $\frac{\partial \psi}{\partial y} = 1$ at 9 equally spaced points along the edge AB and $\psi = 0$ and $\frac{\partial \psi}{\partial n} = 0$, where n is the outward normal along the boundary BC, at 10 equally spaced points along the edge BC. The numerical results of the stream function ψ and the velocity distribution along the center line AC are plotted in Fig. 15, Fig. 16 and Fig. 17 for $\alpha = 30°$, $40°$ and $50°$, respectively. The numerical results of streamline ψ and velocity along the center line AC are also obtained for small angles $\alpha = 10°$ and $20°$.

The numerical results for ψ_{max} and its location are listed in Table 7 for angles $\alpha = 10°$ to $50°$. The boundary errors for stream function and velocity expressed as a percentage of their maximum values are less than 2% and 4.5%, respectively, for angles $\alpha \leq 40°$.

4.4 Creeping Flow in Cavities of Circular Segmental Cross Section

The symmetry of the problem (see Fig. 18) shows that equation (6) can be used for the circular segmental cavity. The coefficients b_i and c_i are determined by satisfying $\psi = 0$ and $\frac{\partial \psi}{\partial y} = 1$ at 9 equally spaced points along the edge AB and $\psi = 0$ $\frac{\partial \psi}{\partial n} = 0$ at 10 equally spaced points along the arc BC. The numerical results of the stream function ψ and velocity distribution along the center line AC are plotted in Fig. 19 and Fig. 20 for $\alpha = 60°$ and $90°$, respectively. The numerical

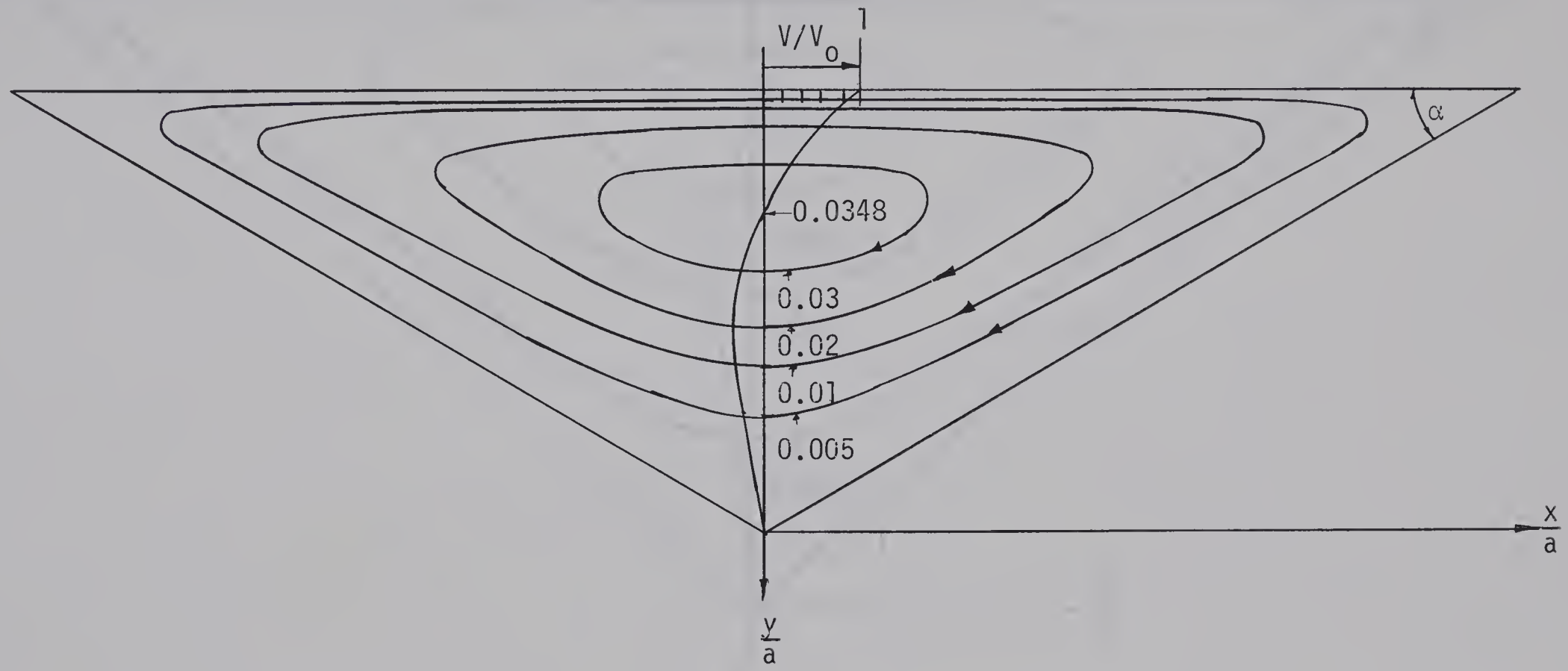

Fig. 15 Creeping flow streamline patterns and velocity distribution along the center line for the triangular cavity for $\alpha = 30°$

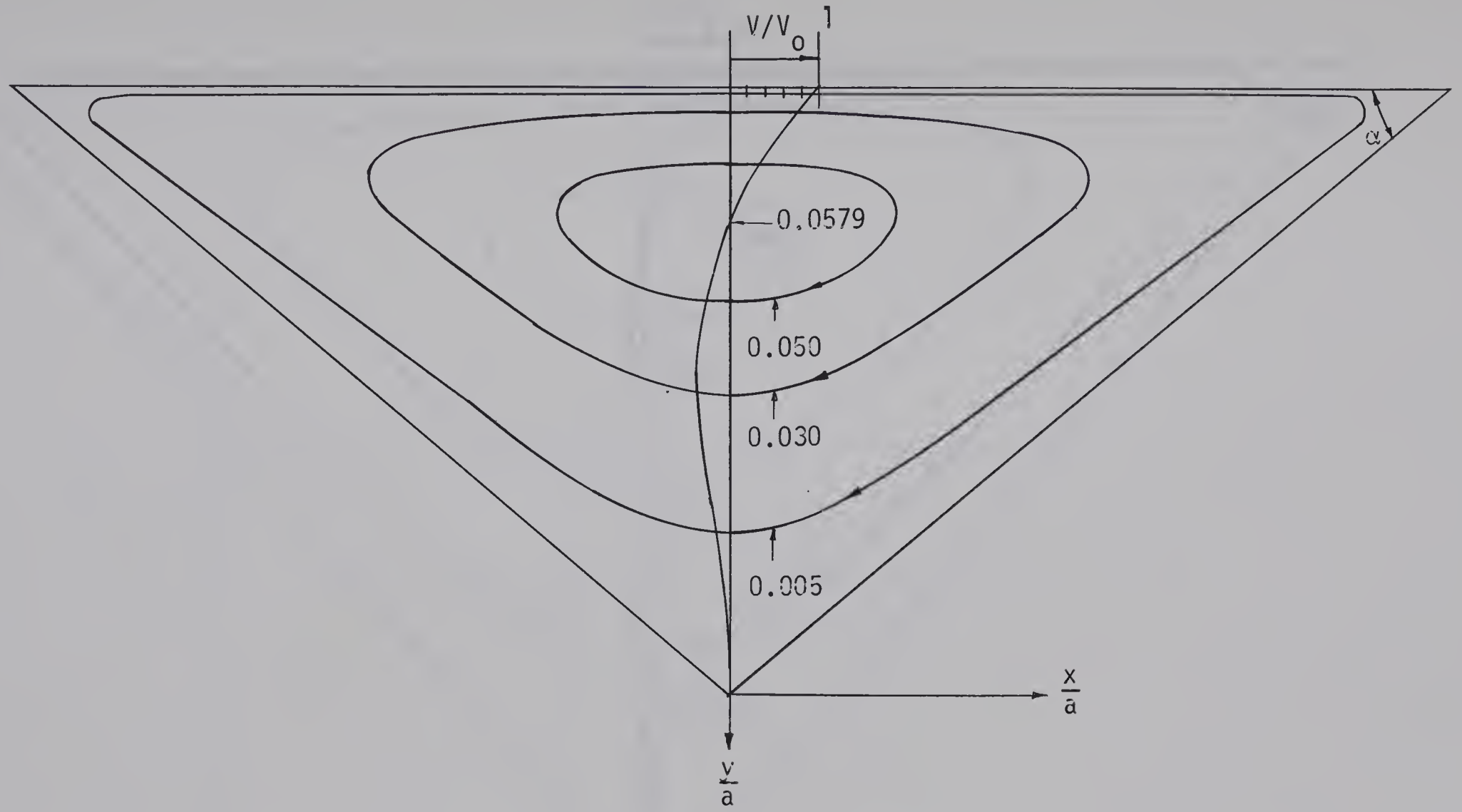

Fig. 16 Creeping flow streamline patterns and velocity distribution along the center line for the triangular cavity for $\alpha = 40°$

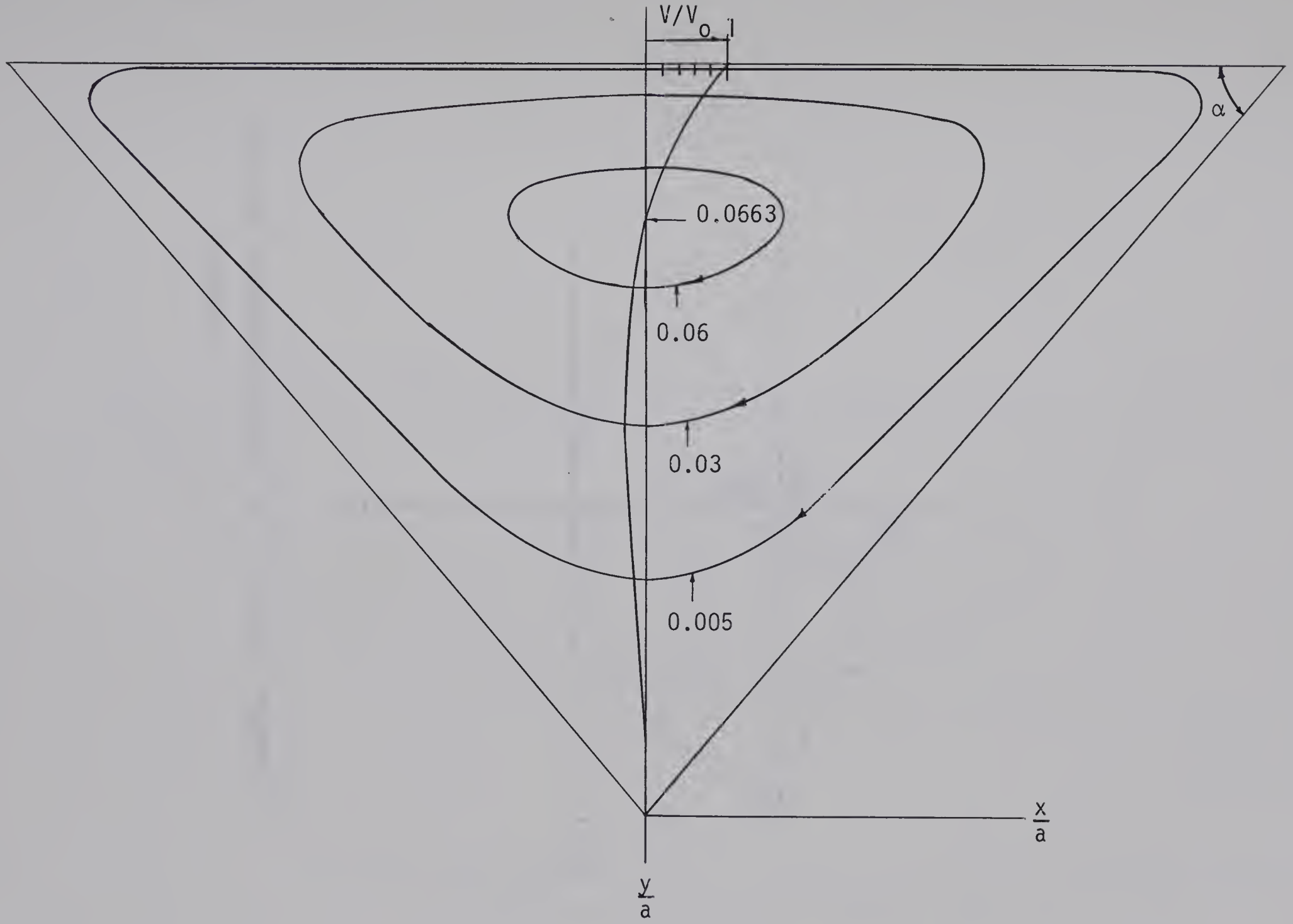

Fig. 17 Creeping flow streamline patterns and velocity distribution along the center line for the triangular cavity for $\alpha = 50°$

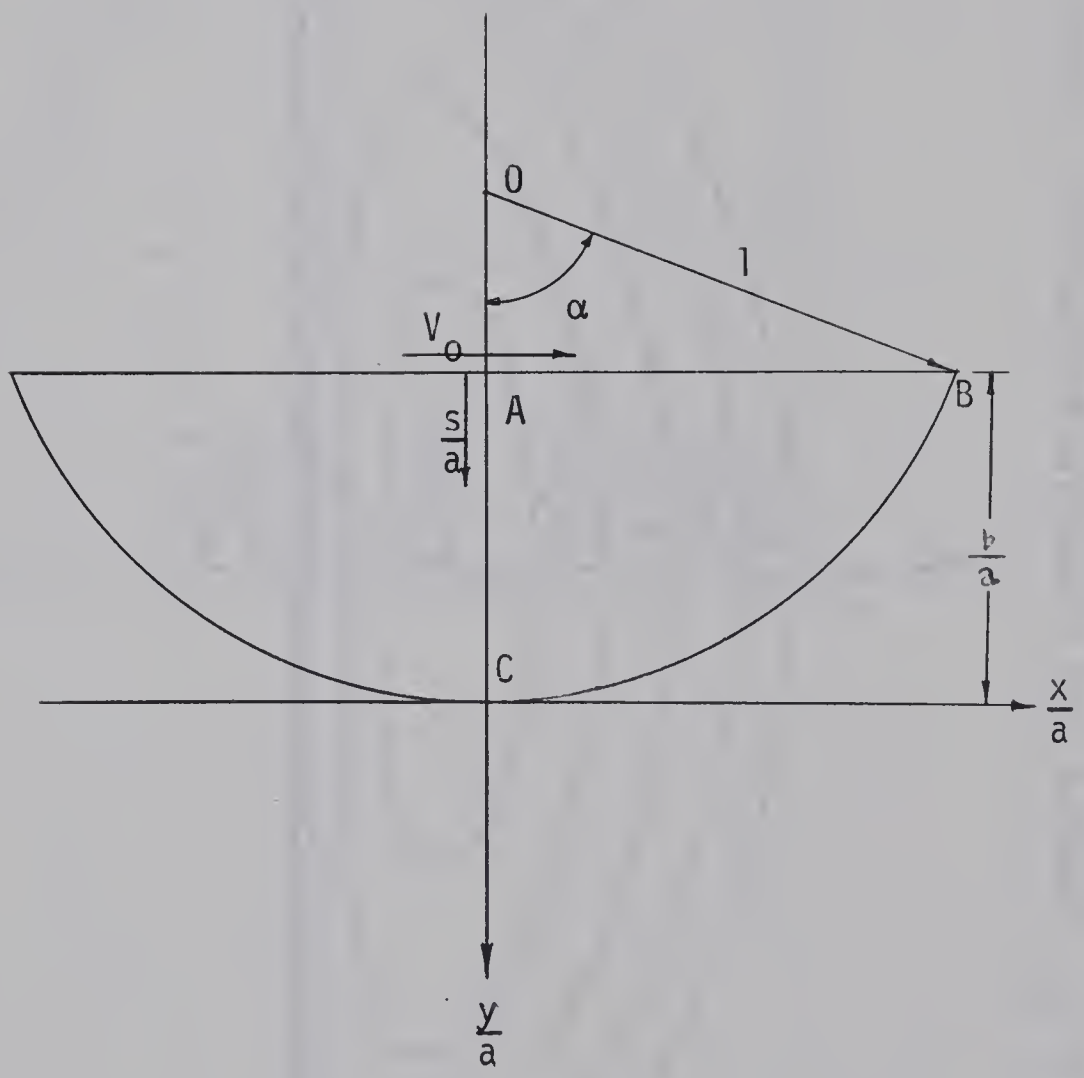

Fig. 18 Coordinate system for a circular segmental cavity

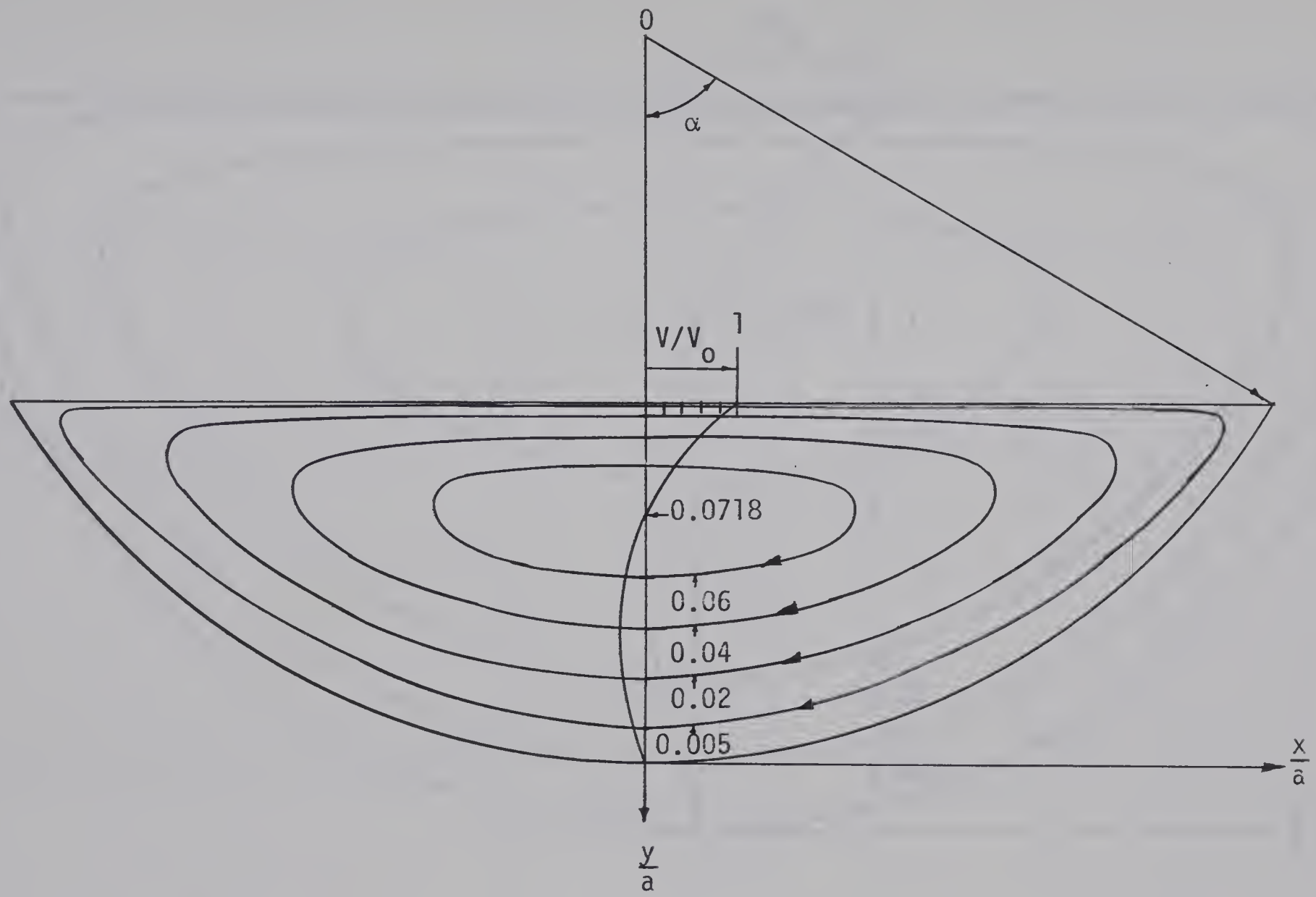

Fig. 19 Creeping flow streamline patterns and velocity distribution along the center line for circular segmental cavity for $\alpha = 60°$

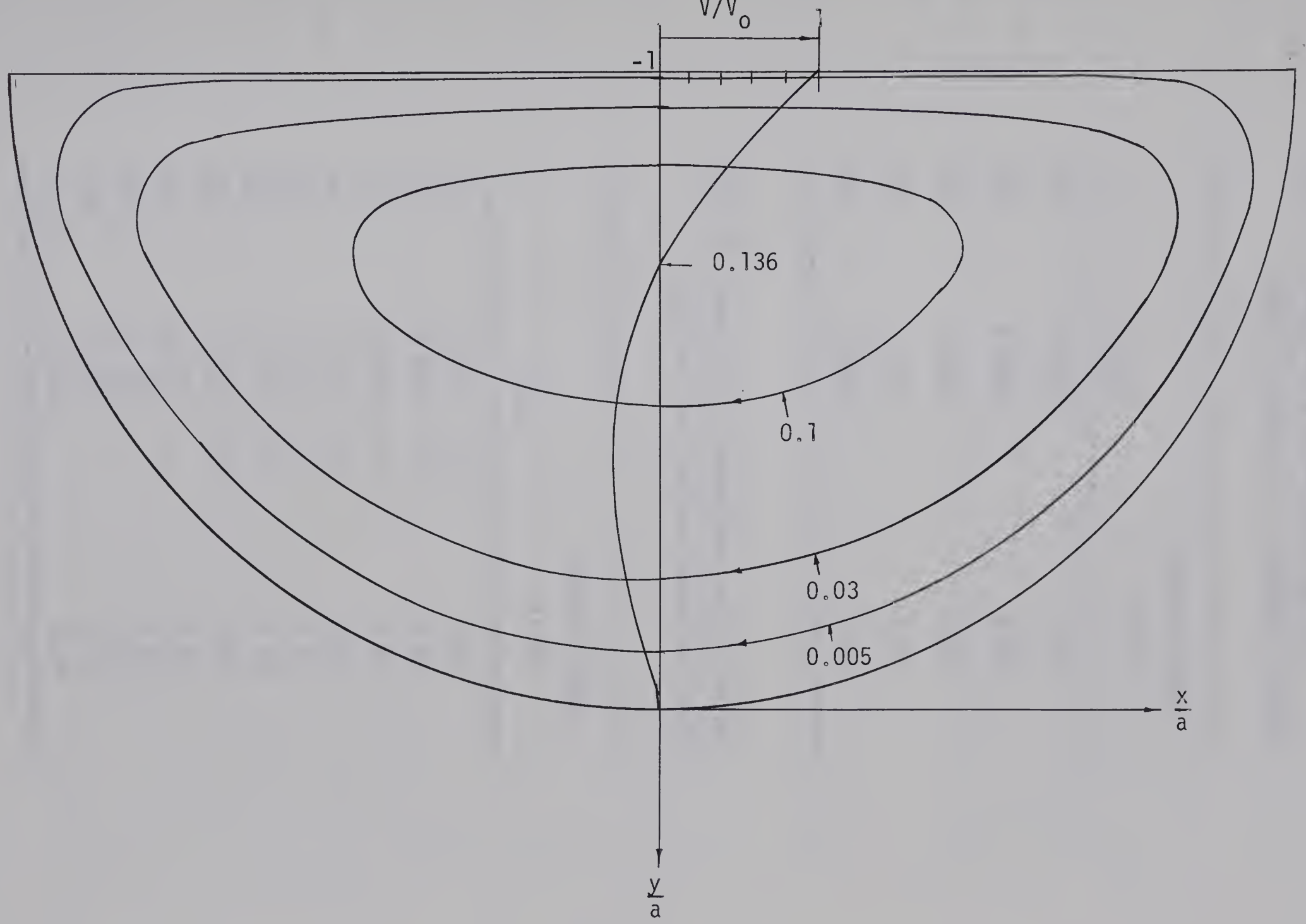

Fig. 20. Creeping flow streamline patterns and velocity distribution along the center line for the circular segmental cavity for $\alpha = 90°$

Table 7 Numerically determined vortex center location in triangular cavity

α	ψ_{max}	Vortex Center (s/b)
10°	0.0126	0.32
20°	0.0242	0.30
30°	0.0350	0.27
40°	0.0579	0.23
50°	0.0663	0.23

Table 8 Numerically determined vortex center location in circular segmental cavity

α	ψ_{max}	Vortex Center (s/b)
10°	0.225×10^{-2}	0.35
20°	0.890×10^{-2}	0.32
30°	0.197×10^{-1}	0.32
40°	0.342×10^{-1}	0.32
50°	0.519×10^{-1}	0.32
60°	0.718×10^{-1}	0.32
70°	0.932×10^{-1}	0.32
80°	0.115	0.32
90°	0.136	0.30
100°	0.155	0.30
110°	0.170	0.30

results of maximum stream function ψ and its location are listed in Table 8 for angles α = 10° to 110°.

The boundary errors for stream function and velocity expressed as a percentage of their maximum values are less than 1.5% and 4%, respectively, for $\alpha \leq 60°$. As the angle α increases from 80° to 110° the boundary errors around the upper corner gradually increase. The maximum boundary errors for velocity is about 7% around the upper corner for α = 70°.

The reason that the large boundary errors for velocity occur in the vicinity of the upper corner for all the creeping flow problems will be discussed next.

The numerical results show that there are large boundary errors for velocity in the region of the upper corner for creeping flow problems due to the discontinuity of the velocity in this corner. It is physically impossible that a velocity field is discontinuous at a certain point since the shear stress should be infinite. Mathematically, the solution of biharmonic equation should be continuous in the second derivative in the whole region of the problem. However, the exact solution of the creeping flow stream function subject to the boundary conditions used must have a discontinuity in its first derivatives at the upper corner E. But the approximate solution is written in terms of a series of g_i and G_i which are continuous in their first derivative (actually continuous up to nth derivative, where n can be any positive integer). Consequently, the error in the first derivative of the approximate solution is large in the neighbourhood of the upper corner.

CHAPTER V

CONCLUDING REMARKS

1. The exact solution in Cartesian coordinates can be used for a class of problems governed by the biharmonic equation, such as uniformly loaded thin plate with all edges clamped and creeping flow problems.
2. The well known general solution of the biharmonic equations in polar coordinates can not be readily applied to problems such as uniformly loaded clamped rectangular plates with large aspect ratios and uniformly loaded clamped rhombus plates with small angles α (see Fig. 1(a) and (b)). In contrast, the general solution of the biharmonic equation in Cartesian coordinates yields the approximate solutions to the above problems readily. However, it is noted that the expressions for the harmonic functions g_i and biharmonic functions G_i become quite involved as the number of terms to be used increases.
3. The numerical results indicate that the point-matching technique can be used for the biharmonic boundary value problems when the boundary conditions are of the Cauchy type, i.e. w and $\frac{\partial w}{\partial n}$ are specified along the boundary. The boundary errors are very small

compared with the maximum values inside the region for most of the clamped plates. However, for the clamped rhombus plate with angles α less than 25° and the clamped circular segmental plate with angles α less than 30°, larger boundary deviations were found.

4. Several problems with boundary conditions other than the Cauchy boundary conditions were attempted using these functions g_i and G_i and the point-matching technique. In most cases boundary errors were large in comparison to the maximum values inside the region. Reasonable results for problems with non-Cauchy type boundary conditions are obtained only in the case of the uniformly loaded, simply supported rhombus plate with angles α = 45° and 40° (see Fig. 1(b)). Numerical results are listed in Table 9, where the boundary conditions $w = 0$ and $M_n = 0$, are satisfied at 9 equally spaced points along edge AB. The boundary errors for deflection and bending moment are less than 0.4% and 1.5%, respectively, compared with the maximum values of the deflection and bending moment inside the plate. When the angle α is 35°, the maximum boundary errors for the deflection and bending moment are approximately 0.6% and 7%, respectively, compared to the maximum values of the deflection and bending moment inside the plate.

It is also found that errors become large when the boundary condition involves the second derivative of the deflection.

Table 9 Maximum Deflection and Bending Moments of a Uniformly Loaded Rhombus Plate With All Edges Simply Supported

degree α	$\left(\frac{w}{\frac{qa^4}{D}}\right)_{(0,0)}$	$\left(\frac{M_x}{qa^2}\right)_{(0,0)}$	$\left(\frac{M_y}{qa^2}\right)_{(0,0)}$
45°	0.16249×10^{-1}	0.95771×10^{-1}	0.95771×10^{-1}
40°	0.22953×10^{-1}	0.11844	0.10916

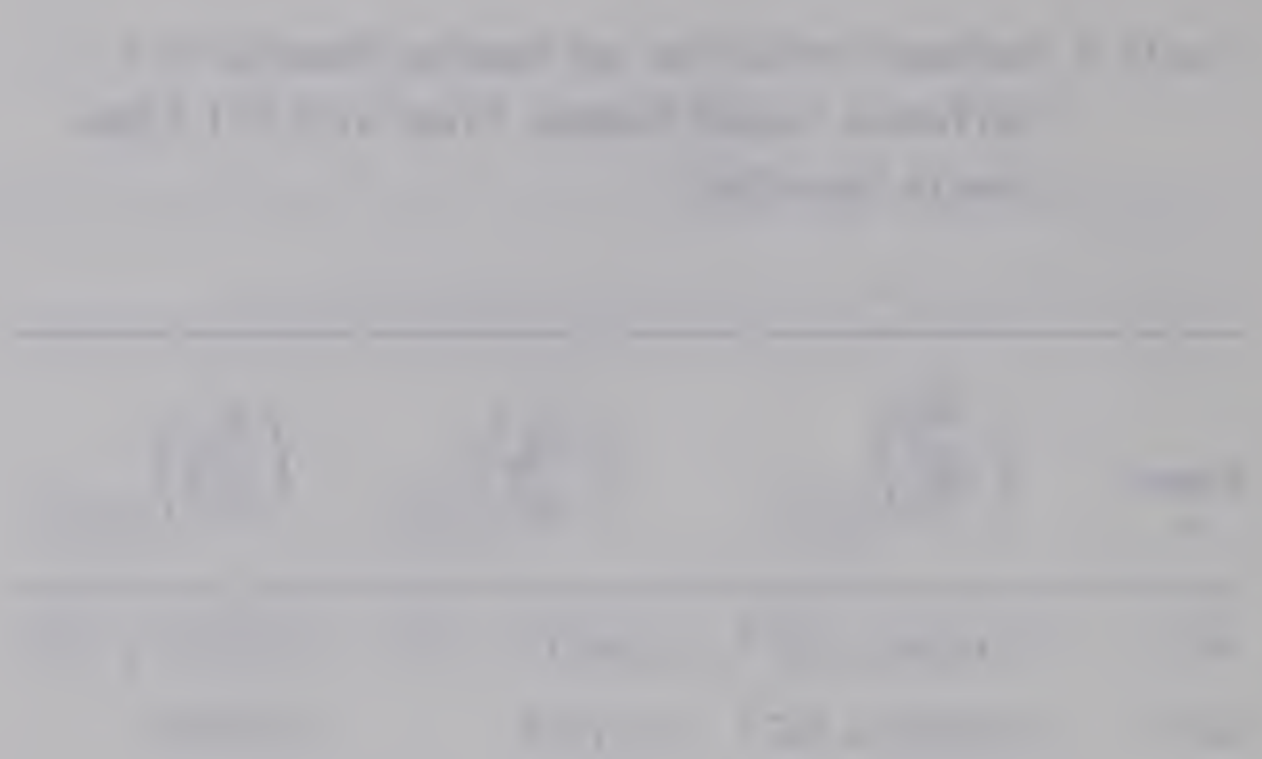

REFERENCES

1. S. Timoshenko and S. Woinowsky-Krieger, "Theory of Plates and Shells", McGraw-Hill Book Company, Inc., New York, 1959.
2. H.D. Conway, "The approximate analysis of certain boundary value problems", Journal of Applied Mechanics, Vol. 27, pp. 275-277, 1960.
3. K.C. Cheng, "Laminar Flow and Heat Transfer Characteristics in Regular Polygonal Ducts", Proceedings of the Third International Heat Transfer Conference A.I.Ch.E., Vol. 1, pp. 64-76, 1966.
4. L.E. Hulbert, "The Numerical Solution of Two-Dimensional Problems of the Theory of Elasticity", Bulletin 198 Engineering Experiment Station, Ohio State University, Columbus, Ohio.
5. C.C. Lo, "The Solution of Plane Harmonic and Biharmonic Boundary Value Problems in the Theory of Elasticity", Ph.D. dissertation, Ohio State University, 1964.
6. C.J. Thorne, "Square Plate Fixed at Points", Journal of Applied Mechanics, Vol. 70, pp. 73-79, 1948.
7. E.M. Sparrow and A. Haji-Sheikh, "Flow and Heat Transfer in Ducts of Arbitrary Shape with Arbitrary Thermal Boundary Conditions", Journal of Heat Transfer, Trans. ASME, Series C, Vol. 88, pp. 351-358, 1966.
8. George C. Feng, "Bending of Elastic Plates with Arbitrary Shapes", Journal of the Engineering Mechanics Division, Proceeding of the ASCE, pp. 5687-5691, Dec., 1967.

9. C.C. Lo and F.W. Niedenfuhr, "On Improving the Convergence of Fourier Series Solutions in Plane Biharmonic Problems", Journal of Applied Mechanics, Vol. 34, Trans. ASME, Vol. 89, Series E, pp. 210-212, 1967.

10. S.S. Sattinger and H.D. Conway, "The Solution of Certain Isosceles Triangle and Rhombus Torsion and Plate Problems", International Journal of Mechanical Sciences, Vol. 7, pp. 221-228, 1965.

11. L.S.D. Morley, "Bending of Clamped Rectilinear Plates", Quart. J. Mech. and Applied Math., Vol. 17, pp. 293-317, 1964.

12. S. Woinowsky-Krieger, "Über die Verwendung von Bipolarkoordinaten zur Losung einiger Problem der Plattenbiegung", Österreichisches Ingenieur-Archiv, XXIV. Band, pp. 47-50, 1956.

13. O.R. Burggraf, "The structure of steady separated flow", Vol. 24, Journal of Fluid Mechanics, pp. 113-151, 1966.

14. Frank Pan and Andreas Acrivos, "Steady Flows in Rectangular Cavities", Journal of Fluid Mechanics, Vol. 28, Part 4, pp. 643-656, 1967.

APPENDIX 1

THE g FUNCTIONS

$g_1 = 1$

$g_2 = x$

$g_3 = y$

$g_4 = x^2 - y^2$

$g_5 = 2xy$

$g_6 = x^3 - 3xy^2$

$g_7 = 3x^2y - y^3$

$g_8 = x^4 + y^4 - 6x^2y^2$

$g_9 = 4x^3y - 4xy^3$

$g_{10} = x^5 - 10x^3y^2 + 5xy^4$

$g_{11} = y^5 - 10y^3x^2 + 5yx^4$

$g_{12} = x^6 - 15x^4y^2 + 15x^2y^4 - y^6$

$g_{13} = 6x^5y + 6xy^5 - 20x^3y^3$

$g_{14} = x^7 - 21x^5y^2 + 35x^3y^4 - 7xy^6$

$g_{15} = 7x^6y - 35x^4y^3 + 21x^2y^5 - y^7$

$g_{16} = x^8 + y^8 - 28x^6y^2 + 70x^4y^4 - 28x^2y^6$

$g_{17} = 8x^7y - 56x^5y^3 + 56x^3y^5 - 8xy^7$

$g_{18} = x^9 - 36x^7y^2 + 126x^5y^4 - 84x^3y^6 + 9\ xy^8$

$g_{19} = 9x^8y - 84x^6y^3 + 126x^4y^5 - 36x^2y^7 + y^9$

$g_{20} = x^{10} - 45x^8y^2 + 210x^6y^4 - 210x^4y^6 + 45x^2y^8 - y^{10}$

$g_{21} = 10x^9y - 120x^7y^3 + 25x^5y^5 - 120x^3y^7 + 10xy^9$

$g_{22} = x^{11} - 55x^9y^2 + 330x^7y^4 - 462x^5y^6 + 165x^3y^8 - 11xy^{10}$

$$g_{23} = 11x^{10}y - 165x^8y^3 + 462x^6y^5 - 330x^4y^7 + 55x^2y^9 - y^{11}$$

$$g_{24} = x^{12} - 66x^{10}y^2 + 495x^8y^4 - 924x^6y^6 + 495x^4y^8 - 66x^2y^{10} + y^{12}$$

$$g_{25} = 12x^{11}y - 220x^9y^3 + 792x^7y^5 - 792x^5y^7 + 220x^3y^9 - 12xy^{11}$$

$$g_{26} = x^{13} - 78x^{11}y^2 + 715x^9y^4 - 1716x^7y^6 + 1287x^5y^8 - 286x^3y^{10} + 13xy^{11}$$

$$g_{27} = 13x^{12}y - 286x^{10}y^3 + 1287x^8y^5 - 1716x^6y^7 + 715x^4y^9 - 78x^2y^{11} + y^{13}$$

$$g_{28} = x^{14} - 19x^{12}y^2 + 1001x^{10}y^4 - 3003x^8y^6 + 3003x^6y^8 - 100x^4y^{10} + 19x^2y^{12} - y^{14}$$

$$g_{29} = 14x^{13}y - 364x^{11}y^3 + 2002x^9y^5 - 3432x^7y^7 + 2002x^5y^9 - 364x^3y^{11} + 14xy^{13}$$

$$g_{30} = x^{15} - 105x^{13}y^2 + 1365x^{11}y^4 - 5005x^9y^6 + 6435x^7y^8 - 3003x^5y^{10} + 455x^3y^{12} - 15xy^{14}$$

$$g_{31} = 15x^{14}y - 455x^{12}y^3 + 3003x^{10}y^5 - 6435x^8y^7 + 5005x^6y^9 - 1365x^4y^{11} + 105x^2y^{13} - y^{15}$$

$$g_{32} = x^{16} - 120x^{14}y^2 + 1820x^{12}y^4 - 8008x^{10}y^6 + 12870x^8y^8 - 8008x^6y^{10} + 1820x^4y^{12} - 120x^2y^{14} + y^{16}$$

$$g_{33} = 16x^{15}y - 560x^{13}y^3 + 4368x^{11}y^5 - 11440x^9y^7 + 11440x^7y^9 - 4368x^5y^{11} + 560x^3y^{13} - 16xy^{15}$$

$$g_{34} = x^{17} - 136x^{15}y^2 + 2380x^{13}y^4 - 12376x^{11}y^6 + 24310x^9y^8 - 19448x^7y^{10} + 6188x^5y^{12} - 680x^3y^{14} + 17xy^{16}$$

$$g_{35} = 17x^{16}y - 680x^{14}y^3 + 6188x^{12}y^5 - 19448x^{10}y^7 + 24310x^8y^9 - 12376x^6y^{11} + 2380x^4y^{13} - 136x^2y^{15} + y^{17}$$

$$g_{36} = x^{18} - 153x^{16}y^2 + 3060x^{14}y^4 - 18564x^{12}y^6 + 43758x^{10}y^8 - 43758x^8y^{10} + 18564x^6y^{12} - 3060x^4y^{14} + 153x^2y^{16} - y^{18}$$

$$g_{37} = 18x^{17}y - 816x^{15}y^3 + 8568x^{13}y^5 - 31824x^{11}y^7 + 48620x^9y^9 - 31824x^7y^{11} + 8568x^5y^{13} - 816x^3y^{15} + 18xy^{17}$$

$$g_{38} = x^{19} - 171x^{17}y^2 + 3876x^{15}y^4 - 27132x^{13}y^6 + 75682x^{11}y^8 - 92378x^9y^{10}$$
$$+ 40388x^7y^{12} - 11628x^5y^{14} + 969x^3y^{16} - 19xy^{18}$$

$$g_{39} = 19x^{18}y - 969x^{16}y^3 + 11628x^{14}y^5 - 40388x^{12}y^7 + 92378x^{10}y^9$$
$$- 75682x^8y^{11} + 27132x^6y^{13} - 3876x^4y^{15} + 171x^2y^{17} - y^{19}$$

$$g_{40} = x^{20} - 190x^{18}y^2 + 4845x^{16}y^4 - 38760x^{14}y^6 + 116070x^{12}y^8 - 184756x^{10}y^{10}$$
$$+ 116070x^8y^{12} - 38760x^6y^{14} + 4845x^4y^{16} - 190x^2y^{18} + y^{20}$$

$$g_{41} = 20x^{19}y - 1140x^{17}y^3 + 15504x^{15}y^5 - 67520x^{13}y^7 + 168060x^{11}y^9$$
$$- 168060x^9y^{11} + 67520x^7y^{13} - 15504x^5y^{15} + 1140x^3y^{17} - 20xy^{19}$$

$$g_{42} = x^{21} - 210x^{19}y^2 + 5985x^{17}y^4 - 54264x^{15}y^6 + 183590x^{13}y^8 - 352816x^{11}y^{10}$$
$$+ 284130x^9y^{12} - 106280x^7y^{14} + 20349x^5y^{16} - 1330x^3y^{18} + 21xy^{20}$$

$$g_{43} = 21x^{20}y - 1330x^{18}y^3 + 20349x^{16}y^5 - 106280x^{14}y^7 + 284130x^{12}y^9$$
$$- 352816x^{10}y^{11} + 18350x^8y^{13} - 54264x^6y^{15} + 5985x^4y^{17} - 210x^2y^{19}$$
$$+ y^{21}$$

$$g_{44} = x^{22} - 231x^{20}y^2 + 7315x^{18}y^4 - 74613x^{16}y^6 + 289870x^{14}y^8 - 636946x^{12}y^{10}$$
$$+ 636946x^{10}y^{12} - 289870x^8y^{14} + 74613x^6y^{16} - 7315x^4y^{18} + 231x^2y^{20}$$
$$- y^{22}$$

$$g_{45} = 22x^{21}y - 1540x^{19}y^3 + 26334x^{17}y^5 - 160544x^{15}y^7 + 467720x^{13}y^9$$
$$- 705632x^{11}y^{11} + 467720x^9y^{13} - 160544x^7y^{15} + 26334x^5y^{17} - 1540x^3y^{19}$$
$$+ 22xy^{21}$$

$$g_{46} = x^{23} - 253x^{21}y^2 + 8855x^{19}y^4 - 100947x^{17}y^6 + 450414x^{15}y^8 - 1104666x^{13}y^{10}$$
$$- 1342578x^{11}y^{12} + 757590x^9y^{14} - 235157x^7y^{16} + 33649x^5y^{18} - 1771x^3y^{20}$$
$$+ 23xy^{22}$$

$$g_{47} = 23x^{22}y - 1771x^{20}y^3 + 33649x^{18}y^5 - 235157x^{16}y^7 + 757590x^{14}y^9$$
$$- 1342578x^{12}y^{11} + 1104666x^{10}y^{13} - 450414x^8y^{15} + 100947x^6y^{17}$$
$$- 8855x^4y^{19} + 253x^2y^{21} - y^{23}$$

$$g_{48} = x^{24} - 276x^{22}y^2 + 10626x^{20}y^4 - 134596x^{18}y^6 + 685571x^{16}y^8$$
$$- 1862256x^{14}y^{10} + 2685156x^{12}y^{12} - 1862256x^{10}y^{14} + 685571x^8y^{16}$$
$$- 134596x^6y^{18} + 10626x^4y^{20} - 276x^2y^{20} + y^{24}$$

$$g_{49} = 24x^{23}y - 2024x^{21}y^3 + 42504x^{19}y^5 - 336104x^{17}y^7 + 1208004x^{15}y^9$$
$$- 2447244x^{13}y^{11} + 2447244x^{11}y^{13} - 1208004x^9y^{15} + 336104x^7y^{17}$$
$$- 42504x^5y^{19} + 2024x^3y^{21} - 24xy^{23}.$$

THE G FUNCTIONS

$$G_1 = x^2 + y^2$$

$$G_2 = x^3 + xy^2$$

$$G_3 = x^2y + y^3$$

$$G_4 = x^4 - y^4$$

$$G_5 = x^3y + xy^3$$

$$G_6 = x^5 - 2x^3y^2 - 3xy^4$$

$$G_7 = 3x^4y + 2x^2y^3 - y^5$$

$$G_8 = (x^6 + y^6) - 5(x^4y^2 + y^4x^2)$$

$$G_9 = x^5y - xy^5$$

$$G_{10} = x^7 - 9x^5y^2 - 5x^3y^4 + 5xy^6$$

$$G_{11} = y^7 - 9x^2y^5 - 5x^4y^3 + 5x^6y$$

$$G_{12} = (x^8 - y^8) + 14(x^2y^6 - x^6y^2)$$

$$G_{13} = 3(x^7y + xy^7) - 7(x^5y^3 + x^3y^5)$$

$$G_{14} = x^9 - 20x^7y^2 + 14x^5y^4 + 28x^3y^6 - 7xy^8$$

$$G_{15} = 7x^8y - 28x^6y^3 - 14x^4y^5 + 20x^2y^7 - y^9$$

$$G_{16} = x^{10} + y^{10} + 42(x^6y^4 + x^4y^6) - 27x^8y^2 + x^2y^8)$$

$$G_{17} = 2(x^9y - xy^9) + 12(x^3y^7 - x^7y^3)$$

$$G_{18} = x^{11} - 35x^9y^2 + 90x^7y^4 + 42x^5y^6 - 75x^3y^8 + 9xy^{10}$$

$$G_{19} = 9x^{10}y - 75x^8y^3 + 42x^6y^5 + 90x^4y^7 - 35x^2y^9 + y^{11}$$

$$G_{20} = x^{12} - 44x^{10}y^2 + 165x^8y^4 - 165x^4y^8 + 44x^2y^{10} - y^{12}$$

$$G_{23} = 11x^{12}y - 154x^{10}y^3 + 297x^8y^5 + 132x^6y^7 - 275x^4y^9 + 54x^2y^{11} - y^{13}$$

$$G_{24} = x^{14} - 65x^{12}y^2 + 429x^{10}y^4 - 429x^8y^6 - 429x^6y^8 + 429x^4y^{10} - 65x^2y^{12} + y^{14}$$

$$G_{27} = 13x^{14}y - 273x^{12}y^3 + 1001x^{10}y^5 - 429x^8y^7 - 1001x^6y^9 + 637x^4y^{11} - 77x^2y^{13} + y^{15}$$

$$G_{28} = x^{16} - 90x^{14}y^2 + 910x^{12}y^4 - 2002x^{10}y^6 + 2002x^6y^{10} - 910x^4y^{12} + 90x^2y^{14} - y^{16}$$

$$G_{31} = 15x^{16}y - 440x^{14}y^3 + 2548x^{12}y^5 - 3432x^{10}y^7 - 1430x^8y^9 + 3640x^6y^{11} - 1260x^4y^{13} + 104x^2y^{15} - y^{17}$$

$$G_{32} = x^{18} - 119x^{16}y^2 + 1700x^{14}y^4 - 6188x^{12}y^6 + 4862x^{10}y^8 + 4862x^8y^{10} - 6188x^6y^{12} + 1700x^4y^{14} - 119x^2y^{16} + y^{18}$$

$$G_{35} = 17x^{18}y - 663x^{16}y^3 + 5508x^{14}y^5 - 13260x^{12}y^7 + 4862x^{10}y^9 + 11934x^8y^{11} - 9996x^6y^{13} + 2244x^4y^{15} - 135x^2y^{17} + y^{19}$$

$$G_{36} = x^{20} - 152x^{18}y^2 + 2907x^{16}y^4 - 15504x^{14}y^6 + 25194x^{12}y^8 - 25194x^8y^{12} + 15504x^6y^{14} - 2907x^4y^{16} + 152x^2y^{18} - y^{20}.$$

APPENDIX 2

$$w_h = \sum_{m=0}^{\infty} \sum_{n=0}^{\infty} a_{mn}\, x^m y^n \tag{A1}$$

$$\nabla^4 w_h = 0$$

$$\left(\frac{\partial^4}{\partial x^4} + 2\,\frac{\partial^4}{\partial x^2 \partial y^2} + \frac{\partial^4}{\partial y^4}\right) \sum_{m=0}^{\infty} \sum_{n=0}^{\infty} a_{mn}\, x^m y^n = 0$$

implying $$\sum_{m=4}^{\infty} \sum_{n=0}^{\infty} a_{mn}\,(m)(m-1)(m-2)(m-3)\, x^{m-4} y^n$$

$$+ 2 \sum_{m=2}^{\infty} \sum_{n=2}^{\infty} a_{mn}\,(m)(m-1)(n)(n-1)\, x^{m-2}\, y^{n-2}$$

$$+ \sum_{m=0}^{\infty} \sum_{n=4}^{\infty} a_{mn}\,(n)(n-1)(n-2)(n-3)\, x^m\, y^{n-4} = 0 \tag{A2}$$

The equation (A2) can be written as:

$$\sum_{k=0}^{\infty} \sum_{\ell=0}^{\infty} [a_{k+4,\ell}\,(k+4)(k+3)(k+2)(k+1) + 2a_{k+2,\ell+2}\,(k+2)(k+1)$$

$$(\ell+2)(\ell+1) + a_{k,\ell+4}\,(\ell+4)(\ell+3)(\ell+2)(\ell+1)]\, x^k y^\ell = 0 \tag{A3}$$

implying $$[a_{k+4,\ell}\,(k+4)(k+3)(k+2)(k+1) + 2a_{k+2,\ell+2}\,(k+2)(k+1)$$

$$(\ell+2)(\ell+1) + a_{k,\ell+4}\,(\ell+4)(\ell+3)(\ell+2)(\ell+1)] = 0 \tag{A4}$$

where $k = 0,1,2,3,\ldots \infty$

$\ell = 0,1,2,3,\ldots \infty$

(iii)

Selecting a finite number of terms, then equation (A1) can be written as:

$$w_h = \sum_{m=0}^{p} \sum_{n=0}^{p} a_{mn} x^m y^n \qquad \text{(A5)}$$

where $m + n \leq p$ and $p \geq 4$.

Then in equation (A4), k and ℓ are

$$k = 0, 1, 2, \ldots (p-4)$$
$$\ell = 0, 1, 2, \ldots (p-4) \qquad \text{but } k + \ell \leq (p-4)$$

The number of equations (A4) is $[(p-3)(p-2)/2]$

For instance, $p = 5$, w_h can be written as:

$$\begin{aligned} w_h = {} & a_{0,0} + a_{1,0}x + a_{0,1}y + a_{2,0}x^2 + a_{1,1}xy + a_{0,2}y^2 \\ & + a_{3,0}x^3 + a_{2,1}x^2y + a_{1,2}xy^2 + a_{0,3}y^3 + a_{4,0}x^4 + a_{3,1}x^3y \\ & + a_{2,2}x^2y^2 + a_{1,3}xy^3 + a_{0,4}y^4 + a_{5,0}x^5 + a_{4,1}x^4y \\ & + a_{3,2}x^3y^2 + a_{2,3}x^2y^3 + a_{4,1}xy^4 + a_{0,5}y^5 \end{aligned} \qquad \text{(A6)}$$

Since $k + \ell \leq 5 - 4 = 1$, then there are three constraint equations (A4) which can be written as:

$$\begin{aligned} 3a_{4,0} + a_{2,2} + a_{0,4} &= 0 \\ 5a_{5,0} + a_{3,2} + a_{1,4} &= 0 \qquad \text{(A7)} \\ a_{4,1} + a_{2,3} + 5a_{0,5} &= 0 \end{aligned}$$

Omitting all the details, equation (A6) after using the constraint equations (A7) can be written as:

$$w_h = \sum_{j=1}^{7} b_j G_j + \sum_{i=1}^{11} c_i g_i$$

where the coefficients b_j's and c_i's are linear combination of a_{mn}'s and all the coefficients b_j's and c_i's are linearly independent.